

SCHOOL OF ELECTRICAL ENGINEERING
AND TELECOMMUNICATIONS

Resource Allocation Design for IRS-empowered 6G Networks

by

Yu Liu

Submitted: October 26, 2026
Supervisor: Assoc.Prof Derrick Wing Kwan Ng

Abstract

This paper studies the problem of secrecy rate maximization in a downlink multi-user multiple-input single-output (MISO) wireless communication system assisted by multiple intelligent reflecting surfaces (IRSs), in the presence of multiple eavesdroppers. Perfect channel state information (CSI) is assumed at the transmitter. To enhance physical-layer security, a joint optimization framework is proposed to simultaneously design the transmit beamforming matrix, artificial noise covariance, and IRS phase shift matrices under total power and unit-modulus constraints.

The transmit-side variables are handled via a Lagrangian penalty reformulation, where the optimality of the beamforming and noise matrices is ensured through the satisfaction of Karush-Kuhn-Tucker (KKT) conditions. The IRS phase shifts are optimized using semidefinite relaxation (SDR) followed by a penalty-based majorization-minimization (MM) procedure, enabling the recovery of discrete unit-modulus IRS configurations. The overall non-convex problem is solved through an alternating optimization (AO) strategy that decouples the variables into tractable subproblems.

The simulation findings confirm the efficacy of the suggested strategy, showcasing substantial enhancements in the max-min secrecy rate across various system configurations.These findings provide design insights for secure and scalable IRS-assisted wireless communication systems envisioned in future 5G and 6G networks.

Acknowledgements

The author would like to express sincere appreciation to Associate Professor Derrick Wing Kwan Ng for his outstanding supervision, insightful feedback, and continuous encouragement throughout the course of this research. His deep expertise in wireless communications and optimization theory has greatly influenced the formulation and refinement of the proposed framework. The author is especially grateful for his patience and motivation during challenging stages of the work, which were critical in overcoming technical hurdles and improving the clarity and rigor of the overall contribution. This research experience under his mentorship has been intellectually enriching and has had a lasting impact on the author's academic development and future aspirations.

Abbreviations

IRS Intelligent Reflecting Surface

CSI Channel State Information

MISO Multiple-input Single-Output

SINR Signal-to-Interference- plus-Noise Ratio

AN Artificial Noise

BS Base Station

KKT Karush-Kuhn-Tucker

PLS Physical Layer Security

MRT Maximum Ratio Transmission

CMA-ES Covariance Matrix Adaptation Evolution Strategy

SCA Successive Convex Approximation

NLoS non-line-of-sight

LoS line-of-sight

CSCG circularly symmetric complex Gaussian

MM Majorization minimization

Contents

Acknowledgements **1**

Abbreviations **2**

Contents **3**

1 Introduction **5**

1.1 Background 5

1.2 Literature Review and Research Gaps 6

1.2.1 Reconfigurable propagation environments and multi-IRS architectures . 6

1.2.2 Physical-layer secrecy, eavesdropper models, and artificial noise 7

1.2.3 Covert transmission and other related security objectives 8

1.2.4 Joint active/passive beamforming and resource allocation 9

1.2.5 Unit-modulus and discrete phase-shift optimization 10

1.2.6 Channel estimation, imperfect CSI, and temporal variation 10

1.2.7 Learning-based and scalable alternatives 11

1.2.8 Synthesis and position of the present work 12

1.3 Method Overview 13

1.4 Contributions Summary 15

2 System Model **16**

2.1 Network Description and Channel Assumptions 16

2.2 IRS Phase Modeling with Discrete Control 18

2.3 Secrecy Rate Formulation 19

2.4 Optimization Problem Formulation 20

3 Proposed Algorithm **22**

3.1 Alternating Optimization Framework 22

3.2 IRS Phase Optimization 26

3.3 Transmit Beamforming Optimization 28

3.4 Artificial Noise Optimization 30

4 Simulation Results and Discussion **34**

4.1 Simulation Setup 34

4.2 Simulation Results 35

4.2.1 Impact of System Configuration 35

4.2.2 Convergence and Parameter Analysis 38

5 Conclusion **40**

6 Appendix **42**

6.1 Derivation of User Rate 42

6.1.1 Trace-Based Reformulation 43

6.1.2 Interference and Artificial Noise Power Expressions 44

6.2 Eavesdropper Achievable Rate Expression 44

Bibliography **46**

Chapter 1

Introduction

1.1 Background

Wireless communication takes place over a broadcast medium, so confidential delivery to legitimate receivers must account for unintended receivers. Higher-layer cryptography remains essential, while physical-layer security (PLS) provides a complementary approach based on the propagation channels and the spatial design of transmitted signals. Multiuser MISO transmitters can combine user-specific beamforming with artificial noise to reduce the information accessible to an eavesdropper. Secure multiuser IRS-aided beamforming has been investigated under both idealized and uncertain CSI assumptions [1, 2, 3].

An intelligent reflecting surface (IRS) contains programmable elements that modify the phase, and sometimes amplitude, of incident electromagnetic waves. Such control offers additional opportunities to strengthen desired links or reshape interference without deploying a conventional amplify-and-forward relay. Fundamental system models and practical constraints are reviewed in [4], while the connection between IRS hardware models and optimization algorithms is surveyed in [5]. The security enhancement of a reflecting surface is not automatic: the same reflected paths may also strengthen eavesdropping links, which makes joint active/passive design important [2, 3].

Multiple geographically separated IRSs provide additional channel-shaping dimensions, although they also increase the number of cascaded links and phase-control variables. Relevant studies include multi-IRS mmWave power optimization [6], UAV-based multi-IRS association and phase design [7], distributed statistical passive beamforming [8], and distributed multi-RIS reflection with timing offsets [9]. Motivated by these advances, this thesis considers a downlink

multiuser MISO transmitter assisted by several passive IRSs in the presence of multiple eavesdroppers. It jointly designs information beamforming, artificial-noise covariance, and phase configurations for a max–min secrecy objective under the stated perfect-CSI model. The literature review below identifies the relevant earlier methods, their different assumptions, and the limitations of the present model.

1.2 Literature Review and Research Gaps

1.2.1 Reconfigurable propagation environments and multi-IRS architectures

A reconfigurable intelligent surface (RIS), also referred to as an intelligent reflecting surface (IRS), changes the propagation environment through programmable electromagnetic responses rather than relying entirely on conventional active relaying. The tutorial in [4] discusses channel models, hardware constraints, CSI acquisition, deployment, and joint active–passive beamforming. The development from electromagnetic models to resource-allocation algorithms was reviewed by Ng and coauthors in [5], whereas the large-surface cellular-IoT analysis of [10] demonstrates how system geometry and the number of reflecting elements enter performance evaluation. Practical phase-codebook limitations and associated open problems are surveyed in [11]. These works establish both the promise of programmable channels and the danger of idealizing passive elements as lossless, continuously tunable, or cost-free.

The effective channel in a multi-IRS network is shaped by the base-station-to-surface and surface-to-receiver links, the placement of each surface, and the coordinated choice of phase configurations. Early studies of distributed passive beamforming with statistical CSI [8] and cooperative reflection in the presence of timing offsets [9] show that geographically separated surfaces do not behave identically to a single co-located aperture. Research on double-IRS-assisted multiuser mmWave communications [12] and on multi-IRS full-duplex links with hardware impairments [13] further emphasizes the coupling between surface configuration, propagation topology, and interference. Independently, multi-IRS placement and link selection have been addressed for mmWave MISO systems [6], UAV-aided networks [7], and IRS size/location decisions [14]. Those network-design problems are complementary to, rather than substitutes for, the present thesis's fixed-topology secrecy optimization.

Multi-point processing provides another reference point. Joint-processing coordinated multipoint with an IRS [15], IRS-aided joint processing with underlaid device-to-device communication [16], and distributed precoding in RIS-aided cell-free MIMO [17] all exploit coordination across spatial resources. More recent work on distributed beamforming for beyond-diagonal RIS architectures [18] and on RIS-aided cell-free performance with learning-based control [19] extends this theme. However, coordinated active access points, beyond-diagonal coupling, and multiple independent passive reflecting surfaces are different architectures. The system considered here uses one multi-antenna base station and multiple passive IRSs, without modeling inter-IRS multiple reflections. Consequently, its channel and optimization models should be compared with the corresponding independent-surface baseline rather than with more general cell-free or coupled-RIS models.

1.2.2 Physical-layer secrecy, eavesdropper models, and artificial noise

Physical-layer security (PLS) exploits differences between legitimate and wiretap channels to limit the information recoverable by an unintended receiver. In a multiuser MISO downlink, the base station can choose user-specific information beams, and an artificial-noise (AN) covariance can expend spatial degrees of freedom to degrade eavesdropping. The resulting secrecy rates depend on the intended user's achievable rate, the assumed decoding capability of an eavesdropper, and the interference and AN observed by each receiver. The appropriate objective can be a sum secrecy rate, a worst-user secrecy rate, or a minimum secrecy rate, and results for these objectives cannot be interchanged automatically.

Two directly relevant foundations are the robust and secure IRS-aided resource-allocation formulation of [2], which jointly treats transmit and passive beamforming under imperfect channel information, and the IRS-enabled secure multiuser MISO resource-allocation study [1]. Security enhancement through IRS control is examined in [20]; in a self-sustainable IRS setting, joint robust beamforming and secure sum-rate maximization is considered in [3]. The latter includes the additional challenge of powering the surface, which is not part of the passive-surface power model in this thesis. The development of a wider class of secure IRS-aided transmit designs is summarized in [21], including distinctions between channel shaping and active beamforming.

The adversary model is central to the interpretation of secrecy gains. Spatially correlated channel uncertainty and multiple-antenna eavesdroppers are studied in [22], while the robust

secrecy design of jointly transmitting and reflecting RIS-aided MIMO links under angular uncertainty is investigated in [23]. The outage-constrained secrecy–energy-efficiency treatment with a multi-antenna eavesdropper [24] and a recent joint beamforming/RIS design against an *active* multi-antenna eavesdropper [25] illustrate that uncertainty, receive-array processing, and adversarial interference require additional constraints or different games. Secrecy results derived with perfect legitimate and eavesdropper CSI are therefore useful as benchmarks, but should not be described as robust to channel-estimation errors or an adaptive attacker without separate analysis.

Artificial noise complements beam steering when nulling all eavesdroppers is infeasible or conflicts with intended-user service. In related systems, robust secure MISO beamforming with rate splitting [26], RIS-enabled rate-splitting secure transmission [27], and IRS-aided secure wireless-powered networks [28] jointly manage desired signals and interference under different physical constraints. Energy efficiency of secure IRS-aided simultaneous wireless information and power transfer is examined in [29], while IRS-assisted MIMOME wiretap energy efficiency is considered in [30]. These papers motivate joint transmit covariance and phase optimization, but differ from the present secrecy-rate maximization problem in their access methods, harvesting requirements, or objective functions. In particular, maximizing secrecy rate does not necessarily minimize radiated power or maximize secrecy energy efficiency.

1.2.3 Covert transmission and other related security objectives

It is also important to distinguish information-theoretic secrecy from covertness and secret-key generation. Secure beamforming seeks to limit how much information an eavesdropper can decode; covert communication seeks to make transmission activity difficult to detect. An IRS-assisted multi-antenna covert beamforming problem is developed in [31], followed by approaches involving detection constraints and prior-probability effects [32], full-duplex information freshness [33], and delay constraints [34]. RIS-aided anti-detection and electromagnetic stealth [35, 36], and an IRS-aided covert network with spatially distributed wardens [37], address related adversarial detection models. They inform possible extensions but cannot by themselves substantiate a secrecy-rate claim.

Similarly, RIS-aided physical-layer key generation under spatial correlation [38], multi-cell key generation [39], and the influence of a malicious RIS on key acquisition [40] use different security metrics from wiretap secrecy rate. Beyond terrestrial links, secure RIS-assisted

satellite propagation under Shadowed-Rician fading [41] further illustrates how channel distributions alter security performance. These strands are included here to situate the proposed secrecy beamforming method within the broader security literature, not to imply that its numerical comparisons cover those tasks.

1.2.4 Joint active/passive beamforming and resource allocation

A central difficulty of IRS-assisted MISO design is that the effective channels depend on the product of active transmit beams and passive surface coefficients. The literature therefore often alternates between optimizing transmit-side matrices and the reflecting configuration. The power-efficient multiuser MISO treatment [42], IRS-assisted green communication framework with convergence and robustness analysis [43], and joint transmit/reflective beamforming for IRS-aided rate-splitting multiple access [44] illustrate different routes to tractable subproblems. Research on energy/spectral-efficiency tradeoffs in RIS-aided multiuser MIMO [45] further shows that improvements in one metric need not imply improvements in all others.

For multi-IRS and distributed scenarios, weighted sum-rate optimization with full-duplex hardware impairments [13], multiuser cellular coordination [16], robust cell-free precoding with backhaul and CSI constraints [46], and joint distributed precoding/beamforming [17] demonstrate that active and passive choices become increasingly coupled as the network grows. Other resource-allocation objectives include multi-objective IRS-SWIPT design [47], max–min fair energy-efficient IRS-aided SWIPT [48], large-IRS scalable SWIPT resource allocation [49], and statistical-QoS energy-efficiency analysis [50]. The specific constraints and utility functions differ, but the general lessons about nonconvexity, feasible initialization, and objective-aware alternating updates transfer to secure multi-IRS designs.

Robust secure resource allocation adds further coupling between uncertain channels, the secrecy-rate objective, and optimization variables. The direct IRS-aided robust secrecy studies [2, 3] are especially important comparators because they account for secrecy and multiuser transmission jointly. The physical-layer-security study in [22] additionally models a multi-antenna eavesdropper and spatially correlated uncertainty. By contrast, the baseline considered in this thesis assumes perfect CSI and jointly optimizes user transmit beamforming, AN covariance, and the phases of several IRSs. Its principal distinguishing feature is this *combination of variables and topology*, not a claim that the individual use of AO, SDR, SCA, or AN is new.

1.2.5 Unit-modulus and discrete phase-shift optimization

Continuous unit-modulus coefficients already define a nonconvex feasible set. Real surfaces may support only a finite phase alphabet, may have amplitude–phase coupling, and may incur switching/control overhead. The multiuser discrete-phase design in [51] is particularly germane: Wu *et al.* study globally optimal resource allocation for IRS-assisted multiuser networks with discrete phase shifts under both perfect and imperfect CSI. Its earlier conference treatment [52] documents the discrete-design direction. These studies provide a benchmark against which approximate phase-recovery procedures should be discussed, while their globally optimal method should not be assumed to solve the present multi-IRS secrecy-plus-AN problem directly.

The codebook and hardware design perspective in [11] complements the discrete-phase optimization problem, whereas phase quantization with beam training [53], channel-dependent codebook selection [11], and the secure RIS key-generation phase design [54] demonstrate that discrete control appears across multiple objectives. Robust beamforming in the presence of transceiver impairments [55] and active-IRS resource allocation [56] warn against interpreting ideal passive phase-only solutions as hardware-agnostic. The present thesis uses a semidefinite lifting, a penalty-based majorization–minimization update, and a deterministic projection to the admissible discrete phases. A relaxed solution's objective is not necessarily attained after projection; feasibility and objective improvement must be checked on the final quantized configuration.

A second set of methods exploits special rank structures. The general rank-one beamforming framework in [57], scalable optimization for large IRS-aided systems [49], and provably convergent robust IRS optimization [43] are instructive for interpreting the use of semidefinite relaxations, penalty terms, and surrogate optimization. In this thesis, an alternating algorithm can be assessed for the monotonicity of the *actual feasible secrecy objective* and for convergence of its objective values; this does not by itself establish a globally optimal discrete phase solution or a KKT point of the original mixed-discrete problem.

1.2.6 Channel estimation, imperfect CSI, and temporal variation

Most joint active/passive resource-allocation models presuppose effective channels that are expensive to obtain. Cascaded channel estimation with quantized beamforming [53], deep

residual network estimation for IRS-assisted multiuser links [58], semi-passive IRS estimation with enhanced deep residual networks [59], and partially decoupled atomic-norm estimation for RIS-aided MIMO [60] explore complementary model-based and learning-based estimators. Semi-blind estimation of RIS-assisted MISO channels [61] and massive access using semi-passive RIS elements [62] further reduce or redistribute pilot and sensing requirements. However, their overhead and assumptions are not interchangeable: semi-passive elements, multiple antennas, prior sparsity, and learning data offer different types of channel knowledge.

Multi-IRS training is additionally sensitive to the number of cascaded paths and the way the surfaces are configured during pilots. Statistical passive beamforming in distributed IRSs [8], partial-CSI RIS-assisted multiuser MIMO [63], and robust cell-free designs with constrained backhaul [46] examine useful alternatives to instantaneous perfect CSI. With user mobility, outdated CSI affects RIS-assisted UAV communications [64], channel aging changes cell-free RIS-aided performance [65], and channel-aging-aware precoding is treated explicitly in [66]. Near-field and large-aperture effects, explored through piecewise channel modeling [67] and sensing-based estimation of extremely large RISs [68], are additional extensions beyond the present far-field narrowband baseline.

For the current thesis, perfect CSI at the transmitter for legitimate and eavesdropper links is a deliberate modeling assumption. It permits a controlled assessment of the secrecy/beamforming tradeoff, but also means that channel acquisition time, eavesdropper CSI uncertainty, training overhead, and the sensitivity of quantized phases to estimation error fall outside its demonstrated results. The robust IRS work [2, 51] and the uncertainty-aware secure work [22] provide natural starting points for a subsequent robust design.

1.2.7 Learning-based and scalable alternatives

Data-driven methods aim to lower online optimization effort or adapt decisions as channels evolve. Predictive multiuser IRS beamforming [69], deep residual channel estimation [58], RIS-aided cell-free optimization using deep reinforcement learning [19], and secure predictive beamforming in sensing-and-communications networks [70] illustrate distinct uses of learning. Reinforcement-learning-based resource allocation, learned channel prediction, and a learned optimizer address different computational bottlenecks; their performance depends on training distributions and implementation costs, and none automatically guarantees secrecy feasibility outside those distributions.

Scalable processing is also studied through energy-efficient RIS-aided cell-free architectures [71], distributed beamforming across nonstandard surfaces [18], and robust resource allocation in active-IRS-aided rate-splitting systems [72]. The low-complexity design of this thesis instead uses a model-based alternating approach. Its runtime should be assessed against both iteration counts and the number of candidate discrete phase configurations, ideally with explicit channel-estimation and control costs in a follow-up implementation study.

Table 1.1: Representative literature and its relationship to the present thesis.

Research strand	**Representative treatment**	**Difference from this thesis**
Secure IRS beamforming [2, 3] [22]	Robust multiuser secrecy, self-sustainable surfaces, or uncertain eavesdropper channels	Here: multiple passive IRSs, AN, and perfect CSI
Multi-IRS coordination [13] [9, 8]	Full-duplex hardware impairments or distributed reflection/timing	Here: secure downlink MISO, no inter-IRS reflection
Discrete-phase IRS design [51] [11]	Global discrete optimization or codebook design	Here: approximate SDR–MM-based recovery for secrecy design
Channel acquisition [60, 59, 53]	Cascaded CSI estimation, semi-passive training, or quantized beams	Here: perfect-CSI benchmark without training overhead
Learning and prediction [69, 58] [19]	Prediction, channel reconstruction, and DRL control	Here: model-based alternating optimization

1.2.8 Synthesis and position of the present work

The reviewed literature establishes five relevant baselines. First, standard IRS channel modeling and deployment work supplies the propagation foundations [4] and extensions to distributed surfaces [8, 9]. Second, robust secure IRS beamforming and secure multiuser MISO formulations address secrecy directly [2, 3] [22]. Third, scalable resource allocation and alternating optimization show how coupled surface and transmitter decisions can be updated [43, 42, 49]. Fourth, discrete phase optimization [51] sets a demanding benchmark for hardware-constrained designs. Fifth, channel-estimation, uncertainty, and channel-aging studies identify deployment

limitations absent from a perfect-CSI analysis [60, 65, 66].

The gap motivating this thesis is therefore *not* an absence of earlier secure IRS systems or of AO/SDR methods. It is the need to examine the joint choice of downlink user beams, artificial-noise covariance, and multiple passive-IRS phase configurations for several legitimate users and eavesdroppers, under the stated perfect-CSI and power assumptions. The proposed algorithm should be judged in terms of its achieved *feasible* max–min secrecy rate and its computational cost relative to appropriate baselines. Robustness to imperfect eavesdropper CSI, channel training, hardware-aware power consumption, coupled inter-surface paths, and formal global optimality remain important extensions rather than claims of the present work.

1.3 Method Overview

The primary objective of this research is to maximize the secrecy rate in a downlink IRS-assisted multi-user wireless communication system. The secrecy rate is defined as the difference between the legitimate user's achievable rate and that of the eavesdropper, and the goal is to maximize this metric by optimizing the following three critical variables: The beamforming matrix for transmission $\mathbf{W}_k$, The covariance matrix of generated noise $\mathbf{V}$, and the IRS phase shift matrix $\boldsymbol{\Theta}$. This optimization must be performed under realistic system constraints, including total transmit power limits and the unit-modulus constraint on the IRS elements. In contrast to prior works focusing on a single centralized IRS, this project extends the model to include multiple spatially distributed IRSs, each independently assisting signal reflection along different links, offering increased spatial flexibility and secrecy enhancement potential.

To accomplish this goal, the research sets out the following specific objectives:

- Reformulate the secrecy rate expression into a trace-based matrix formulation, which expresses the user and eavesdropper rates in terms of matrix traces involving channel components and beamforming variables. This formulation facilitates convex optimization and allows the constraints to be handled more systematically.
- Decompose the joint optimization problem using an AO strategy. Three subproblems are derived from the main non-convex issue, where each variable group $\boldsymbol{\Theta}$, $\mathbf{W}_k$, and $\mathbf{V}$ is optimized while the other two are fixed.

- Optimize the IRS phase shift matrix $\mathbf{\Theta}$, which is constrained to be unit-modulus and indirectly affects both the legitimate and eavesdropper channels through effective channel gains. Because of the rank-one structure in the lifted formulation, this subproblem is extremely non-convex. It is addressed by applying semidefinite relaxation (SDR) followed by a penalty-based Majorization-Minimization (MM) method, which Iteratively minimizes a difference-of-convex (DC) surrogate and uses the nuclear norm to approximate the rank-one constraint. Unlike conventional methods that randomly quantize the relaxed continuous phases, this framework explicitly recovers discrete phase shifts after the MM procedure, ensuring physical realizability and improved performance in practical hardware-constrained IRS deployments.

- Optimize The beamforming matrix for transmit $\mathbf{W}_k$ and The covariance matrix of generated noise $\mathbf{V}$ in an inner-loop alternating fashion. Each subproblem is handled as follows:

  - When optimizing $\mathbf{W}_k$ with fixed $\mathbf{V}$, the secrecy rate objective is first transformed using the Dinkelbach algorithm, which converts the fractional form into a subtractive one. The resulting problem is then tackled via successive convex approximation (SCA) and SDR, relaxing the rank constraint on $\mathbf{W}_k$.

  - When optimizing $\mathbf{V}$ with fixed $\mathbf{W}_k$, a similar approach is applied, utilizing SCA to approximate the non-convex terms and SDR to relax the covariance matrix structure.

- Ensure all subproblems are solved under Karush-Kuhn-Tucker (KKT) condition compliance, which provides theoretical guarantees for local optimality and convergence of the overall alternating optimization procedure.

By achieving these objectives, the project proposes a comprehensive and theoretically grounded optimization framework for enhancing physical-layer secrecy in IRS-assisted wireless systems. Furthermore, the framework accommodates scenarios with multiple IRSs, providing additional degrees of control without requiring inter-IRS coordination or cascade reflection.

The notation $\mathbf{C}^{M\times N}$ indicates a complex matrix of dimensions $M \times N$. The symbol j represents the imaginary unit, satisfying $j^2 = -1$. A circularly symmetric complex Gaussian (CSCG) distribution with mean μ and variance σ^2 is expressed as $\mathcal{CN}(\mu, \sigma^2)$. The identity matrix is

represented by $\mathbf{I}$. For any general matrix $\mathbf{G}$, the following notations are used: $\mathbf{G}^*$ for the conjugate, $\mathbf{G}^T$ for the transpose, $\mathbf{G}^H$ for the conjugate transpose, $\mathrm{Tr}(\mathbf{G})$ for the trace, and $\mathrm{Rank}(\mathbf{G})$ for the rank of $\mathbf{G}$.The Frobenius norm of the matrix $\mathbf{G}$ is represented as $\|\mathbf{G}\|_F$. For every given vector $\mathbf{w}$, $\|\mathbf{w}\|_2$ signifies its Euclidean length, and $\mathrm{diag}(\mathbf{w})$ constructs a square matrix where the entries of $\mathbf{w}$ are placed along the main diagonal. In the context of optimization, the optimal solution for a variable x is indicated by $x^\star$. The symbols $\mathrm{Re}(\cdot)$ and $\lambda(\cdot)$ signify the real portion and the eigenvalue of a complex variable, respectively.

1.4 Contributions Summary

The following is a summary of this work's primary contributions:

- A novel secrecy rate maximization framework is developed for a downlink MISO system assisted by multiple distributed IRSs and subject to multiple eavesdroppers. Unlike existing works that focus on single-IRS or simplified channel conditions, the proposed model considers practical multi-IRS deployment with full channel dependencies.

- The non-convex optimization problem is tackled via an AO procedure. Each variable group—including the transmit beamforming matrix, artificial noise covariance, and IRS phase shifts—is updated iteratively while the others are held fixed.

- For the IRS phase matrices, semidefinite relaxation (SDR) is employed in conjunction with a penalty-based majorization-minimization (MM) approach. The resulting continuous phase solutions are then deterministically projected back to discrete phase values, avoiding random quantization.

- For the transmit beamforming and artificial noise matrices, a Lagrangian-based method is used, incorporating a penalty term to enforce constraints and ensuring convergence to KKT-optimal solutions under the AO framework.

- Extensive simulations are conducted using CVX and Taylor approximation techniques. The results verify the monotonic convergence and demonstrate that increasing the number of IRSs significantly enhances the secrecy performance under various configurations.

Chapter 2

System Model

2.1 Network Description and Channel Assumptions

A protected MISO framework incorporating IRS technology is depicted in Figure 3.1. The system consists of an AP (Alice) with N_t antennas, There are S IRSs, each containing M reflecting elements. The network setup comprises K authorized users, each equipped with a single antenna. $k \in \mathcal{K}$, where $\mathcal{K} = \{1, 2, \ldots, K\}$ along with n unauthorized users, each possessing a sole antenna (Eves). Due to the presence of eavesdroppers in the wireless environment, the transmission rate of legitimate users may decrease due to interference from the eavesdroppers. To reduce the impact of eavesdroppers on the communication system, the AP transmits artificial noise (AN) along with the information signal to interfere with the eavesdroppers' signal reception. This disturbance technique strengthens the protection of the framework by impairing the signal reception experienced by unintended interceptors, thereby improving the confidentiality of the communication. Additionally, the reflection phase θ of the IRS can be optimized to further improve the received signal quality for legitimate users while reducing the signal strength received by the eavesdroppers, thus maximizing the secrecy of the channel in the MISO system.

The transmitted signal consists of the precoding matrix , the information-bearing signal and synthetic interference (AN) defined as

$$\boldsymbol{X} = \sum_{k=1}^{k} \mathbf{w}_k S_k + \boldsymbol{v} \tag{2.1}$$

where $\mathbf{w}_k \in \mathbf{C}^{N_t \times k}$ and $S_k \in \mathbf{C}$ denote the precoding matrix and the information-bearing signal, respectively, with $S_k \sim \mathcal{CN}(0,1)$, $\forall k \in \mathcal{K}$. $\boldsymbol{v} \in \mathbf{C}^{N_t \times 1}$ denotes the artificial noise (AN) vector, which follows A complicated distribution of Gaussian$\boldsymbol{v} \sim \mathcal{CN}(0, \boldsymbol{V} \succeq 0)$, where $\boldsymbol{V}$ represents

the covariance matrix of $\boldsymbol{v}$. It is necessary for $\boldsymbol{V}$ to be a semi-positive definite matrix to ensure that the artificial noise power is non-negative.

The transmit and interference beamforming vectors should satisfy the following constraint

$$\sum_{k=1}^{k} \|\mathbf{w}_k\|^2 + \mathrm{Tr}(V) \leq P_{\max} \tag{2.2}$$

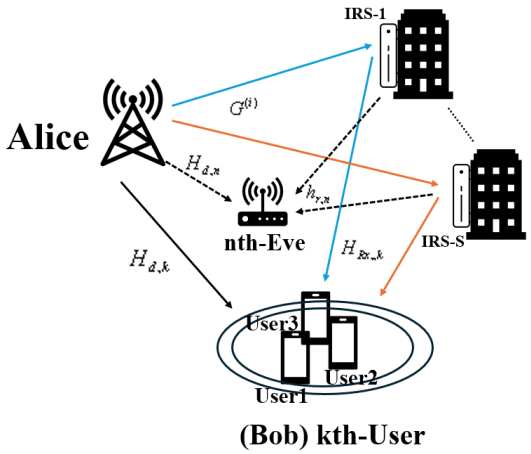


Figure 2.1: Modeling of Multi-IRS-Assisted MISO System

The received signal at legitimate user k can be expressed as

$$\boldsymbol{y_k} = \sum_{k=1}^{K} H_{d,k}^H X + \sum_{i=1}^{S} \sum_{k=1}^{K} H_{Rx,k,i}^H \tilde{\Theta}_i G_i X + n_k \tag{2.3}$$

Let $\boldsymbol{H}_{d,k}$ denote the channel matrix from the base station (AP) to the legitimate user k, with dimension $\boldsymbol{H}_{d,k} \in \mathbb{C}^{N_t \times 1}$. $\boldsymbol{H}_{\mathrm{Rx},k,i}$ represents the channel matrix from the i-th IRS panel to the legitimate user k, and its dimension is $\boldsymbol{H}_{\mathrm{Rx},k,i} \in \mathbb{C}^{M \times 1}$. $\boldsymbol{G}_i$ represents the channel gain between the access point (AP) and the i-th IRS module, with dimension $\boldsymbol{G}_i \in \mathbb{C}^{M \times N_t}$. $\tilde{\boldsymbol{\Theta}}_i$ represents the reflection phase of the i-th IRS, where $\tilde{\boldsymbol{\Theta}}_i \in \mathbb{C}^{M \times M}$ for $i \in \{1, \ldots, S\}$.
The random Gaussian disturbance observed at user k is represented by $n_k \sim \mathcal{CN}(0, \sigma^2)$.

Assuming that all CSI can be accurately obtained at the base stations, leveraging advanced and efficient channel estimation techniques. For instance, CSI can be derived at various base

stations by utilizing pilot signals received from users, with manageable training overhead. According to formula 3.2, the SINR of k users as follows.

$$\mathrm{SINR}_k = \frac{\left|\sum_{i=1}^{S}\left(H_{Rx,k,i}^H \tilde{\Theta}_i G_i + H_{d,k}^H\right)\mathbf{w}_k\right|^2}{\sum_{\substack{j=1\\ j\neq k}}^{K}\left|\sum_{i=1}^{S}\left(H_{Rx,j,i}^H \tilde{\Theta}_i G_i + H_{d,j}^H\right)\mathbf{w}_j\right|^2 + \left|\sum_{i=1}^{S}\left(H_{Rx,k,i}^H \tilde{\Theta}_i G_i + H_{d,k}^H\right)v\right|^2 + \sigma^2} \tag{2.4}$$

To evaluate the secrecy performance, several assumptions are made regarding eavesdropper capabilities. First, eavesdroppers are unable to cancel multi-user interference, and are assumed to adopt passive strategies without emitting detectable signals. In scenarios with multiple eavesdroppers, no cooperation is assumed among them. Furthermore, each eavesdropper experiences additive Gaussian noise similar to legitimate users [1].

The n-th eavesdropper's obtained signal is represented as

$$y_{E,n} = \sum_{n=1}^{n} h_{d,n}^H(\mathbf{w}_k S_k + v) + \sum_{i=1}^{S}\sum_{n=1}^{n} h_{r,n,i}^H \tilde{\Theta}_i G_i(\mathbf{w}_k S_k + v) + n_e \tag{2.5}$$

where $h_{d,n} \in \mathbb{C}^{N_t \times 1}$ denotes the direct channel from the base station, $h_{r,n,i} \in \mathbb{C}^{m\times 1}$ is the IRS-to-eavesdropper channel, $G_i \in \mathbb{C}^{m\times N_t}$ is the AP-to-IRS channel, and θ_i is the IRS reflection matrix. The noise n_e is modeled as $\mathcal{CN}(0,\sigma_e^2)$.

To simplify representation, define an effective channel:

$$H_{E,n,i} = \mathrm{diag}(h_{r,n,i}^H)G_i, \quad h_{n,i}^H = f^H H_{E,n,i} + h_{d,n}^H$$

where $f = [f_1,\ldots,f_m]^H$ and $f_m = e^{j\theta_m}$ captures the IRS phase shifts [51].

The resulting SINR at the n-th eavesdropper is expressed as

$$\mathrm{SINR}_{E,n} = \frac{\left|\sum_{i=1}^{S} h_{n,i}^H \mathbf{w}_k\right|^2}{\sum_{j=1,j\neq n}^{K}\left|\sum_{i=1}^{S} h_{n,i}^H \mathbf{w}_j\right|^2 + \left|\sum_{i=1}^{S} h_{n,i}^H v\right|^2 + \sigma_e^2} \tag{2.6}$$

2.2 IRS Phase Modeling with Discrete Control

For an IRS system with a single base station, a simplified reflection model can be adopted to optimize the phase response of each reflecting element. In this design, the IRS allows each of

its reflecting elements to be activated in a binary manner, determining whether it participates in phase shifting.

The assignment vector for the M reflective elements is represented as $A = [a_1, \ldots, a_M]^T \in \{1\}^M$, where each $a_m = 1$ indicates that the m-th reflecting element is active and allowed to fully adjust its phase shift within $[0, 2\pi]$. This setup ensures that all elements contribute to beamforming, thus providing full phase control capability for the IRS. [73].

The ideal continuous phase-shift vector is denoted by $\phi = [\phi_1, \ldots, \phi_M]^T$, with each $\phi_m \in [0, 2\pi]$. The effective phase-shift vector, represented as $\angle\theta$, is defined as:

$$\angle\theta = \phi \odot A$$

where $\odot$ denotes element-wise multiplication. The final reflection phase shift vector is then given by:

$$\tilde{\Theta} = e^{j\angle\theta}$$

To accommodate hardware constraints in practical IRS implementations, each ideal continuous phase ϕ_m is projected onto a predefined discrete phase set using a Majorization-Minimization (MM)-based recovery procedure. Unlike conventional methods relying on random rounding, this approach deterministically selects the nearest discrete phase value for each element, ensuring better secrecy performance under discrete control limitations.

2.3 Secrecy Rate Formulation

This section begins by defining the system performance metrics, followed by the formulation of the secrecy rate maximization problem based on the resource allocation strategy within the described multi-IRS MISO framework.

The information leakage rate at the n-th eavesdropper is defined as

$$R_{E,n} = \log_2(1 + \mathrm{SINR}_{E,n}) \tag{2.7}$$

$$R_{E,n} = \log_2 \left(1 + \frac{\left| \sum_{i=1}^{S} \left(\mathbf{f}^H \operatorname{diag}(\mathbf{h}_{\mathrm{r},n,i}^H) \mathbf{G}_i + \mathbf{h}_{d,n}^H \right) \mathbf{w}_k \right|^2}{\sum_{\substack{j=1 \\ j \neq k}}^{K} \left| \sum_{i=1}^{S} \left(\mathbf{f}^H \operatorname{diag}(\mathbf{h}_{\mathrm{r},n,i}^H) \mathbf{G}_i + \mathbf{h}_{d,n}^H \right) \mathbf{w}_j \right|^2 + \left| \sum_{i=1}^{S} \left(\mathbf{f}^H \operatorname{diag}(\mathbf{h}_{\mathrm{r},n,i}^H) \mathbf{G}_i + \mathbf{h}_{d,n}^H \right) \mathbf{v} \right|^2 + \sigma_e^2} \right)$$

The k-th valid user's attainable rate is provided by

$$R_k = \log_2(1 + \mathrm{SINR}_k) \tag{2.8}$$

$$R_k = \log_2 \left(1 + \frac{\left| \sum_{i=1}^{S} \left(\mathbf{H}_{\mathrm{Rx},k,i}^H \tilde{\Theta}_i \mathbf{G}_i + \mathbf{H}_{d,k}^H \right) \mathbf{w}_k \right|^2}{\sum_{\substack{j=1 \\ j \neq k}}^{K} \left| \sum_{i=1}^{S} \left(\mathbf{H}_{\mathrm{Rx},j,i}^H \tilde{\Theta}_i \mathbf{G}_i + \mathbf{H}_{d,j}^H \right) \mathbf{w}_j \right|^2 + \left| \sum_{i=1}^{S} \left(\mathbf{H}_{\mathrm{Rx},k,i}^H \tilde{\Theta}_i \mathbf{G}_i + \mathbf{H}_{d,k}^H \right) \mathbf{v} \right|^2 + \sigma^2} \right)$$

The instantaneous secrecy rate for user k is thus expressed as [1][2]

$$R_k^{\mathrm{User}} = R_k - R_{E,n} \tag{2.9}$$

2.4 Optimization Problem Formulation

Considering the worst-case eavesdropper, the effective secrecy rate is defined by

$$R_k^{\mathrm{User}'} \leq \left[R_k - \max_{n' \in \mathcal{N}} \{ R_{E,n'} \} \right]^+ \tag{2.10}$$

$$\left[R_k^{\mathrm{User}} \right]^+ = \max(R_k^{\mathrm{User}}, 0) \tag{2.11}$$

The objective is to maximize the minimum effective secrecy rate among all users while satisfying power and design constraints. The optimization problem is formulated as:

$$\begin{aligned}
&\underset{\{\mathbf{W}_k\}, \tilde{\Theta}, \mathbf{V}, \tau_{n,k}}{\text{maximize}} && \tau_{n,k} \\
&\text{subject to} && \tau_{n,k} \leq R_k^{\text{user'}}, \quad \forall k && \text{(2.11a)} \\
& && \sum_{k=1}^{K} \|\mathbf{w}_k\|^2 + \mathrm{Tr}(\mathbf{V}) \leq P_{\max} && \text{(2.11b)} \\
& && \tilde{\Theta} = e^{j \angle \boldsymbol{\theta}} && \text{(2.11c)} \\
& && \angle \boldsymbol{\theta}_m = \boldsymbol{\phi} \odot \mathbf{A}, \quad \forall m && \text{(2.11d)} \\
& && \phi_m \in [0, 2\pi], \quad \forall m && \text{(2.11e)} \\
& && a_m \in \{1\}, \quad \forall m && \text{(2.11f)} \\
& && \mathbf{V} \succeq 0 && \text{(2.11g)}
\end{aligned}$$

Constraint (2.11a) ensures that the auxiliary variable $\tau_{n,k}$ does not exceed the secrecy rate R_k^{User} of legitimate user k, thereby guaranteeing the minimum secrecy performance of the system. Constraint (2.11b) imposes a total transmit power constraint, stating that the combined power of all beamforming vectors $\mathbf{w}_k$ and the artificial noise covariance matrix $\boldsymbol{V}$ must not exceed the maximum allowable power $P_{\max}$ [56]. Constraints (2.11c)–(2.11e) describe the IRS phase control structure, where each reflecting element reflects the signal with a uniform amplitude and has a phase ϕ_m belonging to $[0, 2\pi]$. Constraint (2.11d) expresses the coupling between the IRS phase and its activation status through the Hadamard product $\boldsymbol{\phi} \odot \boldsymbol{A}$. However, since all reflecting elements are assumed to be active in this study, constraint (2.11f) fixes $a_m = 1$ for all m, eliminating any switch-off operation. It is worth noting that the IRS phase variable ϕ_m is not directly selected from a discrete set. Instead, it is first optimized in the continuous domain using a majorization–minimization (MM) approach and then projected onto a discrete phase set to meet hardware implementation requirements. Finally, constraint (2.11g) ensures that the artificial noise covariance matrix $\boldsymbol{V}$ is positive semidefinite, allowing effective jamming of eavesdroppers without degrading the performance of legitimate users[47].

Chapter 3

Proposed Algorithm

3.1 Alternating Optimization Framework

This section presents an alternating optimization (AO) framework designed to solve the secrecy rate maximization problem formulated in the previous section. Owing to the fundamental non-convex structure of the initial formulation—primarily arising from coupled variables and fractional objectives—the problem is decomposed into several subproblems, each focusing on a distinct subset of variables. Specifically, the optimization variables are divided into three groups: beamforming vectors, artificial noise covariance matrices, and IRS phase shift matrices. These groups are updated iteratively in an alternating manner while fixing the remaining variables.[74]

To handle the non-convexity in each subproblem, several convexification and approximation techniques are employed. Semidefinite relaxation (SDR) is used to deal with rank-one constraints in the beamforming design.[75] Successive convex approximation (SCA) is adopted to linearize non-convex terms around the current solution. [76]The fractional objective function is handled using the Dinkelbach method, which transforms the problem into a series of subtractive convex programs. For the discrete phase shift constraint of the IRS, the majorization–minimization (MM) technique is applied to project the solution onto the feasible discrete set.[55]

Each subproblem is either convex or admits a tractable convex approximation, and satisfies the Karush–Kuhn–Tucker (KKT) conditions.[77] This ensures that the original non-convex problem's stationary point is reached using the suggested AO method. The complete structure

of the iterative optimization procedure is illustrated in the figure below.

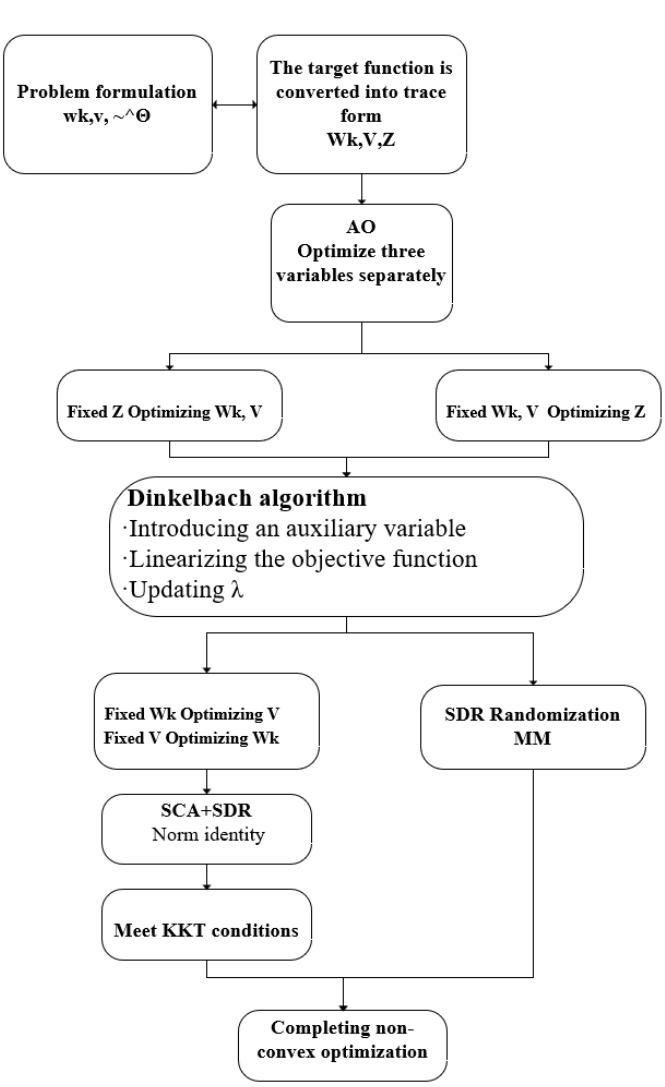


Figure 3.1: Overall optimization framework of the proposed algorithm.

The flowchart illustrates the overall structure of the proposed optimization algorithm. The process begins with problem reformulation and variable separation via AO. Then, the Dinkelbach algorithm is used to convert the fractional secrecy objective into a subtractive form. The IRS phase shift subproblem is handled using SDR and MM, while the transmit beamforming and artificial noise subproblems are solved via SCA and SDR under KKT conditions.

To facilitate the mathematical tractability of the optimisation problem and prepare for the application of semidefinite relaxation (SDR) and successive convex approximation (SCA), the received signal power terms are reformulated into quadratic forms expressed via the trace op-

erator. Define $\mathbf{W}_k = \mathbf{w}_k \mathbf{w}_k^H$, with $\text{Rank}(\mathbf{W}_k) = 1$. Define $\mathbf{V} = \mathbf{v}\mathbf{v}^H$, with $\text{Rank}(\mathbf{V}) = 1$.

Let the composite channel representation associated with user k be denoted as:

$$\boldsymbol{F}_k = \begin{bmatrix} \text{diag}(\boldsymbol{H}_{Rx,k,i}^H)\boldsymbol{G}_i \\ \boldsymbol{H}_{d,k}^H \end{bmatrix} \in \mathbb{C}^{(M+1)\times N_t}, \tag{3.1}$$

where $\boldsymbol{G}_i \in \mathbb{C}^{M\times N_t}$ denotes the channel from the base station to the i-th IRS panel, $\boldsymbol{H}_{Rx,k,i} \in \mathbb{C}^{M\times 1}$ represents the IRS-to-user k reflected path, and $\boldsymbol{H}_{d,k} \in \mathbb{C}^{N_t\times 1}$ is the direct link between the base station and user k.

The augmented IRS reflection vector is defined as:

$$\boldsymbol{z}_i = \begin{bmatrix} \tilde{\boldsymbol{z}}_i \\ 1 \end{bmatrix}, \quad \text{where} \quad \tilde{\boldsymbol{z}}_i = [\theta_1, \theta_2, \ldots, \theta_M]^T \in \mathbb{C}^{M\times 1}. \tag{3.2}$$

By substituting the above-defined extended channel matrix and augmented IRS phase vector into the received signal model, the key terms in the SINR expression can be transformed into trace-based quadratic forms. These are given as:

$$\left| \sum_{i=1}^{S} \left(\mathbf{H}_{\text{Rx},k,i}^H \tilde{\boldsymbol{\Theta}}_i \mathbf{G}_i + \mathbf{H}_{d,k}^H \right) \mathbf{w}_k \right|^2 = \sum_{i=1}^{S}\sum_{l=1}^{S} \text{Tr}\left((\mathbf{z}_i^H \mathbf{F}_k)\, \mathbf{W}_k\, (\mathbf{F}_k^H \mathbf{z}_l) \right)$$

$$\sum_{\substack{j=1 \\ j\neq k}}^{K} \left| \sum_{i=1}^{S} \left(\mathbf{H}_{\text{Rx},j,i}^H \tilde{\boldsymbol{\Theta}}_i \mathbf{G}_i + \mathbf{H}_{d,j}^H \right) \mathbf{w}_j \right|^2 = \sum_{\substack{j=1 \\ j\neq k}}^{K}\sum_{i=1}^{S}\sum_{l=1}^{S} \text{Tr}\left((\mathbf{z}_i^H \mathbf{F}_k)\, \mathbf{W}_j\, (\mathbf{F}_k^H \mathbf{z}_l) \right)$$

$$\left| \sum_{i=1}^{S} \left(\mathbf{H}_{\text{Rx},k,i}^H \tilde{\boldsymbol{\Theta}}_i \mathbf{G}_i + \mathbf{H}_{d,k}^H \right) \mathbf{v} \right|^2 = \sum_{i=1}^{S}\sum_{l=1}^{S} \text{Tr}\left((\mathbf{z}_i^H \mathbf{F}_k)\, \mathbf{V}\, (\mathbf{F}_k^H \mathbf{z}_l) \right)$$

In a similar manner, the signal components received by the eavesdropper can also be reformulated using the trace representation. The extended channel model and IRS phase vector structure defined previously are equally applicable in this context.

$$\left| \sum_{i=1}^{S} \left(\mathbf{f}^H \,\text{diag}(\mathbf{h}_{\text{r},n,i}^H) \mathbf{G}_i + \mathbf{h}_{d,n}^H \right) \mathbf{w}_k \right|^2 = \sum_{i=1}^{S}\sum_{l=1}^{S} \text{Tr}\left((\mathbf{z}_i^H \mathbf{F}_{\text{eve},n}) \mathbf{W}_k (\mathbf{F}_{\text{eve},n}^H \mathbf{z}_l) \right)$$

$$\sum_{\substack{j=1 \\ j\neq k}}^{K} \left| \sum_{i=1}^{S} \left(\mathbf{f}^H \,\text{diag}(\mathbf{h}_{\text{r},n,i}^H) \mathbf{G}_i + \mathbf{h}_{d,n}^H \right) \mathbf{w}_j \right|^2 = \sum_{\substack{j=1 \\ j\neq k}}^{K}\sum_{i=1}^{S}\sum_{l=1}^{S} \text{Tr}\left((\mathbf{z}_i^H \mathbf{F}_{\text{eve},n}) \mathbf{W}_j (\mathbf{F}_{\text{eve},n}^H \mathbf{z}_l) \right)$$

$$\left| \sum_{i=1}^{S} \left(\mathbf{f}^H \operatorname{diag}(\mathbf{h}_{\mathrm{r},n,i}^H) \mathbf{G}_i + \mathbf{h}_{d,n}^H \right) \mathbf{v} \right|^2 = \sum_{i=1}^{S} \sum_{l=1}^{S} \operatorname{Tr} \left((\mathbf{z}_i^H \mathbf{F}_{\mathrm{eve},n}) \mathbf{V} (\mathbf{F}_{\mathrm{eve},n}^H \mathbf{z}_l) \right)$$

Where:

$$\mathbf{h}_{E,n,i} = \operatorname{diag}(\mathbf{h}_{r,n,i}^H) \mathbf{G}_i$$

$$\mathbf{h}_{n,i}^H = \mathbf{f}^H \mathbf{h}_{E,n,i} + \mathbf{h}_{d,n}^H$$

Define the extended channel matrix:

$$\mathbf{F}_{\mathrm{eve},n} = \begin{pmatrix} \mathbf{h}_{E,n,i} \\ \mathbf{h}_{d,k}^H \end{pmatrix}$$

Based on the above derivations, the received signal power for both legitimate users and eavesdroppers is reformulated using trace operations, facilitating a compact representation of the objective function and constraints in the subsequent optimization process. Specifically, a weighting factor λ is introduced to balance the trade-off between enhancing legitimate communication and suppressing eavesdropping capability in the optimization objective.

$$\begin{aligned} \max_{\{\mathbf{W}_k\}, \mathbf{V}, \{\mathbf{Z}_i\}} \quad & \log_2(1+\gamma_k) - \lambda^{(t)} \log_2(1+\gamma_{E,n}) \\ \text{s.t.} \quad & \sum_{k=1}^{K} \operatorname{Tr}(\mathbf{W}_k) + \operatorname{Tr}(\mathbf{V}) \le P_{\max} \\ & \mathbf{W}_k \succeq 0, \quad \forall k \\ & \mathbf{V} \succeq 0 \\ & \mathbf{Z}_i \succeq 0, \quad \forall i \\ & \operatorname{diag}(\mathbf{Z}_i) = \mathbf{1}_{M+1}, \quad \forall i \end{aligned}$$

Where:

$$\mathbf{Z}_i = \mathbf{z}_i \mathbf{z}_i^H$$

$$\gamma_k = \frac{\sum_{i=1}^{S} \sum_{l=1}^{S} \operatorname{Tr} \left(\left(\mathbf{z}_i^H \mathbf{F}_k \right) \mathbf{W}_k \left(\mathbf{F}_k^H \mathbf{z}_l \right) \right)}{\sum_{\substack{j=1 \\ j \neq k}}^{K} \sum_{i=1}^{S} \sum_{l=1}^{S} \operatorname{Tr} \left(\left(\mathbf{z}_i^H \mathbf{F}_k \right) \mathbf{W}_j \left(\mathbf{F}_k^H \mathbf{z}_l \right) \right) + \sum_{i=1}^{S} \sum_{l=1}^{S} \operatorname{Tr} \left(\left(\mathbf{z}_i^H \mathbf{F}_k \right) \mathbf{V} \left(\mathbf{F}_k^H \mathbf{z}_l \right) \right) + \sigma^2}$$

$$\gamma_{E,n} = \frac{\sum_{i=1}^{S}\sum_{j=1}^{S} \mathrm{Tr}\left(\left(\mathbf{z}_i^H \mathbf{F}_{\mathrm{eve},n}\right)\mathbf{W}_k\left(\mathbf{F}_{\mathrm{eve},n}^H \mathbf{z}_l\right)\right)}{\sum_{\substack{j=1\\ j\neq k}}^{K}\sum_{i=1}^{S}\sum_{l=1}^{S} \mathrm{Tr}\left(\left(\mathbf{z}_i^H \mathbf{F}_{\mathrm{eve},n}\right)\mathbf{W}_j\left(\mathbf{F}_{\mathrm{eve},n}^H \mathbf{z}_l\right)\right) + \sum_{i=1}^{S}\sum_{l=1}^{S} \mathrm{Tr}\left(\left(\mathbf{z}_i^H \mathbf{F}_{\mathrm{eve},n}\right)\mathbf{V}\left(\mathbf{F}_{\mathrm{eve},n}^H \mathbf{z}_l\right)\right) + \sigma_e^2}$$

3.2 IRS Phase Optimization

The IRS phase shifts are optimized when the fabricated noise and transmit beamforming matrices are fixed. To deal with the unit-modulus constraint, the IRS vector is lifted to a rank-one semidefinite matrix $\mathbf{Z}_i = \mathbf{z}_i \mathbf{z}_i^H$. The objective function involving the user and eavesdropper SINR is expressed as a difference of two logarithmic trace terms:

$$\max_{\mathbf{Z}_i} f(\mathbf{Z}_i) = \log_2\left(1 + \frac{\sum_{i=1}^{S}\mathrm{Tr}\left(\mathbf{A}_i^{(k)}\mathbf{Z}_i\right)}{\sum_{i=1}^{S}\mathrm{Tr}\left(\mathbf{B}_i^{(k)}\mathbf{Z}_i\right)+\sigma^2}\right) - \lambda^{(t)}\log_2\left(1 + \frac{\sum_{i=1}^{S}\mathrm{Tr}\left(\mathbf{A}_i^{(E)}\mathbf{Z}_i\right)}{\sum_{i=1}^{S}\mathrm{Tr}\left(\mathbf{B}_i^{(E)}\mathbf{Z}_i\right)+\sigma_e^2}\right)$$

Where:

$$\mathbf{A}_i^{(k)} = \mathbf{F}_k \mathbf{W}_k \mathbf{F}_k^H$$

$$\mathbf{B}_i^{(k)} = \sum_{\substack{j=1\\ j\neq k}}^{K} \mathbf{F}_k \mathbf{W}_j \mathbf{F}_k^H + \mathbf{F}_k \mathbf{V} \mathbf{F}_k^H$$

$$\mathbf{A}_i^{(E)} = \mathbf{F}_{\mathrm{eve},n} \mathbf{W}_k \mathbf{F}_{\mathrm{eve},n}^H$$

$$\mathbf{B}_i^{(E)} = \sum_{\substack{j=1\\ j\neq k}}^{K} \mathbf{F}_{\mathrm{eve},n} \mathbf{W}_j \mathbf{F}_{\mathrm{eve},n}^H + \mathbf{F}_{\mathrm{eve},n} \mathbf{V} \mathbf{F}_{\mathrm{eve},n}^H$$

To address the non-convexity of the fractional SINR expressions, first-order Taylor expansion is applied to linearize the objective function. For a fixed IRS matrix $\mathbf{Z}_i^{(t)}$ at iteration t, the user-side SINR is approximated as:

$$\log_2(1+\gamma_k(\mathbf{Z}_i)) \approx \log_2\left(1+\gamma_k^{(t)}\right) + \frac{1}{\ln 2(1+\gamma_k^{(t)})}\cdot\Delta_k, \tag{3.3}$$

where

$$\gamma_k^{(t)} = \frac{\nu_k^{(t)}}{d_k^{(t)}}, \quad \nu_k^{(t)} = \sum_{i=1}^{S}\mathrm{Tr}\left(\mathbf{A}_i^{(k)}\mathbf{Z}_i^{(t)}\right),$$

$$d_k^{(t)} = \sum_{i=1}^{S}\mathrm{Tr}\left(\mathbf{B}_i^{(k)}\mathbf{Z}_i^{(t)}\right) + \sigma^2,$$

and the linear increment:

$$\Delta_k = \sum_{i=1}^{S}\left[\frac{1}{d_k^{(t)}}\mathrm{Tr}\left(\mathbf{A}_i^{(k)}(\mathbf{Z}_i - \mathbf{Z}_i^{(t)})\right) - \frac{\nu_k^{(t)}}{(d_k^{(t)})^2}\mathrm{Tr}\left(\mathbf{B}_i^{(k)}(\mathbf{Z}_i - \mathbf{Z}_i^{(t)})\right)\right]. \tag{3.4}$$

Similarly, the eavesdropper-side SINR is linearized as:

$$\log_2(1+\gamma_e(\mathbf{Z}_i)) \approx \log_2\left(1+\gamma_e^{(t)}\right) + \frac{1}{\ln 2(1+\gamma_e^{(t)})} \cdot \Delta_e, \tag{3.5}$$

where

$$\gamma_e^{(t)} = \frac{\nu_e^{(t)}}{d_e^{(t)}}, \quad \nu_e^{(t)} = \sum_{i=1}^{S} \mathrm{Tr}\left(\mathbf{A}_i^{(E)}\mathbf{Z}_i^{(t)}\right),$$
$$d_e^{(t)} = \sum_{i=1}^{S} \mathrm{Tr}\left(\mathbf{B}_i^{(E)}\mathbf{Z}_i^{(t)}\right) + \sigma_e^2,$$

and the increment:

$$\Delta_e = \sum_{i=1}^{S}\left[\frac{1}{d_e^{(t)}}\mathrm{Tr}\left(\mathbf{A}_i^{(E)}(\mathbf{Z}_i - \mathbf{Z}_i^{(t)})\right) - \frac{\nu_e^{(t)}}{(d_e^{(t)})^2}\mathrm{Tr}\left(\mathbf{B}_i^{(E)}(\mathbf{Z}_i - \mathbf{Z}_i^{(t)})\right)\right]. \tag{3.6}$$

To promote the rank-one structure of the lifted IRS matrix $\mathbf{Z}_i$, a nuclear norm–based penalty is introduced under the majorization–minimization (MM) framework. This enables semidefinite relaxation followed by structured rank-one recovery.

Specifically, the MM subproblem is formulated as:

$$\begin{aligned} \max_{\mathbf{Z}_i} \quad & \gamma_k(\mathbf{Z}_i) - \frac{1}{2\mu}\sum_{i=1}^{S}(\|\mathbf{Z}_i\|_* - \|\mathbf{Z}_i\|_2) \\ \text{s.t.} \quad & \mathbf{Z}_i \succeq 0, \\ & \mathrm{diag}(\mathbf{Z}_i) = \mathbf{1}_{M+1}, \quad \forall i \end{aligned}$$

Here, $\|\cdot\|_*$ denotes the nuclear norm, and $\|\cdot\|_2$ the spectral norm. The parameter $\mu > 0$ controls the penalty weight. At each MM iteration, the spectral norm is majorised via the dominant eigenvector:

$$\|\mathbf{Z}_i\|_2 \approx \mathrm{Tr}\left(\mathbf{u}_i^{(t)}\mathbf{u}_i^{(t)H}\mathbf{Z}_i\right),$$

where $\mathbf{u}_i^{(t)}$ is the principal eigenvector of $\mathbf{Z}_i^{(t)}$. After convergence, the rank-one solution is extracted as

$$\mathbf{z}_i = \mathrm{eigvec}_{\max}(\mathbf{Z}_i^*), \quad \boldsymbol{\theta}_i = \mathrm{diag}\left([\mathbf{z}_i^*]_{1:M}\right),$$

thus enabling the recovery of a discrete-phase IRS reflection vector from the semidefinite matrix solution.

3.3 Transmit Beamforming Optimization

With fixed IRS phase shifts and artificial noise, the beamforming matrix for each user is optimized by transforming the secrecy rate objective via Dinkelbach's algorithm. The interference coupling causes the resultant issue to stay non-convex.

Successive convex approximation (SCA) is employed to linearize the non-convex components, while semidefinite relaxation (SDR) addresses the rank constraint. The norm identity is utilized to enable a tractable convex reformulation.

For user:

$$\begin{aligned} \max_{\mathbf{W}_k} \quad & \gamma_k' = \log_2(1+\alpha_k) \\ \text{s.t.} \quad & \alpha_k \leq \frac{\mathrm{Tr}(\mathbf{A}_k \mathbf{W}_k)}{B_k} \\ & \mathbf{W}_k \succeq 0 \\ & \sum_{k=1}^{K} \|\mathbf{W}_k\|^2 + \mathrm{Tr}(\mathbf{V}) \leq P_{\max} \end{aligned}$$

Where:

$$\mathbf{A}_k = \sum_{i=1}^{S} \sum_{l=1}^{S} \left(\mathbf{z}_i^H \mathbf{F}_k\right) \cdot \left(\mathbf{F}_k^H \mathbf{z}_l\right)$$

$$B_k = \sum_{\substack{j=1 \\ j \neq k}}^{K} \sum_{i=1}^{S} \sum_{l=1}^{S} \mathrm{Tr}\left(\left(\mathbf{z}_i^H \mathbf{F}_k\right) \mathbf{W}_j \left(\mathbf{F}_k^H \mathbf{z}_l\right)\right) + \sum_{i=1}^{S} \sum_{l=1}^{S} \mathrm{Tr}\left(\left(\mathbf{z}_i^H \mathbf{F}_k\right) \mathbf{V} \left(\mathbf{F}_k^H \mathbf{z}_l\right)\right) + \sigma^2$$

For Eavesdroppers:

$$\begin{aligned} & \gamma_{E,n}' = \log_2(1+\beta_k) \\ \text{s.t.} \quad & \beta_k \leq \frac{\mathrm{Tr}(\mathbf{C}_e \mathbf{W}_k)}{D_e} \\ & \mathbf{W}_k \succeq 0 \\ & \sum_{k=1}^{K} \|\mathbf{W}_k\|^2 + \mathrm{Tr}(\mathbf{V}) \leq P_{\max} \end{aligned}$$

Where:

$$\mathbf{C}_e = \sum_{i=1}^{S}\sum_{l=1}^{S}\left(\mathbf{z}_i^H\mathbf{F}_{\text{eve},n}\right)\cdot\left(\mathbf{F}_{\text{eve},n}^H\mathbf{z}_l\right)$$

$$D_e = \sum_{\substack{j=1\\ j\neq k}}^{K}\sum_{i=1}^{S}\sum_{l=1}^{S}\text{Tr}\left(\left(\mathbf{z}_i^H\mathbf{F}_{\text{eve},n}\right)\mathbf{W}_j\left(\mathbf{F}_{\text{eve},n}^H\mathbf{z}_l\right)\right) + \sum_{i=1}^{S}\sum_{l=1}^{S}\text{Tr}\left(\left(\mathbf{z}_i^H\mathbf{F}_{\text{eve},n}\right)\mathbf{V}\left(\mathbf{F}_{\text{eve},n}^H\mathbf{z}_l\right)\right)+\sigma_e^2$$

Lagrange with respect to Wk :

$$\mathcal{L} = \left(\gamma_k' - \lambda^{(t)}\gamma_{E,n}'\right) - \mu\left(\sum_{k=1}^{K}\|\mathbf{W}_k\|^2 + \text{Tr}(\mathbf{V}) - P_{\max}\right) - \sum_k \text{Tr}(\mathbf{Y}\mathbf{W}_k) - \text{Tr}(\mathbf{X}\mathbf{V})$$

Gradient of Lagrange with respect to Wk :

$$\nabla_{\mathbf{W}_k}\mathcal{L} = -\mu\mathbf{I}_k + \eta\frac{\text{Tr}(\mathbf{A}_k\mathbf{W}_k)}{B_k} + \zeta\frac{\text{Tr}(\mathbf{C}_e\mathbf{W}_k)}{D_e} - \mathbf{Y}$$

Table 3.3: Notation for Lagrangian Gradient w.r.t. $\mathbf{W}_k$

Symbol	Description
μ	Lagrange multiplier for the total power constraint
η	Multiplier associated with the user rate constraint
ζ	Multiplier associated with the eavesdropper rate constraint
$\mathbf{I}_k$	Identity matrix matching the dimension of $\mathbf{W}_k$
$\mathbf{A}_k$	Composite channel matrix related to the legitimate user
$\mathbf{C}_e$	Composite channel matrix related to the eavesdropper
B_k	Interference-plus-noise power at user k
D_e	Interference-plus-noise power at eavesdropper n
$\mathbf{Y}$	Dual variable associated with $\mathbf{W}_k \succeq 0$

Let the gradient of the Lagrangian with respect to $\mathbf{W}_k$ be zero:

$$\mathbf{Y} = -\mu\mathbf{I}_k + \eta\frac{\text{Tr}(\mathbf{A}_k\mathbf{W}_k)}{B_k} + \zeta\frac{\text{Tr}(\mathbf{C}_e\mathbf{W}_k)}{D_e}$$

To establish that the Lagrange multiplier matrix $\mathbf{Y}$ satisfies $\text{rank}(\mathbf{Y}) = N_t - 1$, consider the following derivation.

The optimal transmit beamforming matrix $\mathbf{W}_k$ satisfies the rank-one constraint:

$$\mathbf{W}_k = \mathbf{w}_k \mathbf{w}_k^H, \quad \mathbf{W}_k \succeq 0.$$

According to the complementary slackness condition:

$$\mathbf{Y}\mathbf{W}_k = 0 \quad \Rightarrow \quad \mathbf{Y}\mathbf{w}_k \mathbf{w}_k^H = 0 \quad \Rightarrow \quad \mathbf{W}_k \in \text{Null}(\mathbf{Y}).$$

This implies:

$$\dim(\text{Null}(\mathbf{Y})) \geq 1 \quad \Rightarrow \quad \text{rank}(\mathbf{Y}) \leq N_t - 1.$$

Assume by contradiction that $\dim(\text{Null}(\mathbf{Y})) \geq 2$. Then, there exists a vector $\mathbf{u} \notin \text{span}(\mathbf{w}_k)$ such that $\mathbf{Y}\mathbf{u} = 0$. Construct the perturbed matrix:

$$\widetilde{\mathbf{W}}_k = \mathbf{w}_k \mathbf{w}_k^H + \varepsilon \mathbf{u}\mathbf{u}^H, \quad \varepsilon > 0.$$

Since $\mathbf{Y}\mathbf{u} = 0$, it holds that $\text{Tr}(\mathbf{Y}\widetilde{\mathbf{W}}_k) = 0$, and $\widetilde{\mathbf{W}}_k \succeq 0$, meaning the KKT conditions are still satisfied. However, $\widetilde{\mathbf{W}}_k$ has a higher rank than $\mathbf{W}_k$, contradicting the uniqueness and optimality of the rank-one solution.

Therefore,

$$\text{rank}(\mathbf{Y}) = N_t - 1.$$

3.4 Artificial Noise Optimization

When both the IRS phase shifts and the transmit beamforming are fixed, the artificial noise covariance matrix $\mathbf{V}$ is optimized. Again, Dinkelbach's algorithm is used to convert the secrecy rate into subtractive form, followed by SCA and SDR.

For user:

$$\begin{aligned} \max_{\mathbf{V}} \quad & \gamma_k'' = \log_2(1+\rho) \\ \text{s.t.} \quad & \rho \leq \frac{J_k}{\alpha_k(\mathbf{V})} \\ & \mathbf{V} \succeq 0 \\ & \sum_{k=1}^{K} \|\mathbf{W}_k\|^2 + \text{Tr}(\mathbf{V}) \leq P_{\max} \end{aligned}$$

Where:

$$J_k = \sum_{i=1}^{S}\sum_{l=1}^{S} \mathrm{Tr}\left[\left(\mathbf{z}_i^{\mathrm{H}}\mathbf{F}_k\right)\mathbf{W}_k\left(\mathbf{F}_k^{\mathrm{H}}\mathbf{z}_l\right)\right]$$

$$\alpha_k(\mathbf{V}) = \sum_{\substack{j=1\\ j\neq k}}^{K}\sum_{i=1}^{S}\sum_{l=1}^{S} \mathrm{Tr}\left(\left(\mathbf{z}_i^{\mathrm{H}}\mathbf{F}_k\right)\mathbf{W}_j\left(\mathbf{F}_k^{\mathrm{H}}\mathbf{z}_l\right)\right) + \sum_{i=1}^{S}\sum_{l=1}^{S} \mathrm{Tr}\left(\left(\mathbf{z}_i^{\mathrm{H}}\mathbf{F}_k\right)\mathbf{V}\left(\mathbf{F}_k^{\mathrm{H}}\mathbf{z}_l\right)\right) + \sigma^2$$

For Eavesdroppers:

$$\begin{aligned} \max_{\mathbf{V}} \quad & \gamma''_{E,n} = \log_2(1+\psi) \\ \text{s.t.} \quad & \psi \leq \frac{Q_e}{\beta_e(\mathbf{V})} \\ & \mathbf{V} \succeq 0 \\ & \sum_{k=1}^{K} \|\mathbf{W}_k\|^2 + \mathrm{Tr}(\mathbf{V}) \leq P_{\max} \end{aligned}$$

Where:

$$Q_e = \sum_{i=1}^{S}\sum_{l=1}^{S} \mathrm{Tr}\left(\left(\mathbf{z}_n^{\mathrm{H}}\mathbf{F}_{\mathrm{eve},n}\right)\mathbf{W}_k\left(\mathbf{F}_{\mathrm{eve},n}^{\mathrm{H}}\mathbf{z}_l\right)\right),$$

$$\beta_e(\mathbf{V}) = \sum_{\substack{j=1\\ j\neq k}}^{K}\sum_{i=1}^{S}\sum_{l=1}^{S} \mathrm{Tr}\left(\left(\mathbf{z}_i^{\mathrm{H}}\mathbf{F}_{\mathrm{eve},n}\right)\mathbf{W}_j\left(\mathbf{F}_{\mathrm{eve},n}^{\mathrm{H}}\mathbf{z}_l\right)\right) + \sum_{i=1}^{S}\sum_{l=1}^{S} \mathrm{Tr}\left(\left(\mathbf{z}_i^{\mathrm{H}}\mathbf{F}_{\mathrm{eve},n}\right)\mathbf{V}\left(\mathbf{F}_{\mathrm{eve},n}^{\mathrm{H}}\mathbf{z}_l\right)\right) + \sigma_e^2$$

Lagrange with respect to V :

$$\mathcal{L} = \left(\gamma''_k - \lambda^{(t)}\gamma''_{E,n}\right) - \mu\left(\sum_{k=1}^{K}\|\mathbf{W}_k\|^2 + \mathrm{Tr}(\mathbf{V}) - P_{\max}\right) + \left(\frac{J_k}{\alpha_k(\mathbf{V})} - \rho\right)\delta + \left(\frac{Q_e}{\beta_e(\mathbf{V})} - \psi\right)\xi - \sum_k \mathrm{Tr}(\mathbf{Y}\mathbf{W}_k) - \mathrm{Tr}(\mathbf{X}\cdot\mathbf{V})$$

Gradient of Lagrange with respect to V :

$$\nabla_{\mathbf{V}}\mathcal{L} = -\mu\mathbf{V} - \frac{J_k}{\alpha_k(\mathbf{V})^2}\cdot\delta\cdot\frac{\partial\alpha_k(\mathbf{V})}{\partial\mathbf{V}} - \frac{Q_e}{\beta_e(\mathbf{V})^2}\cdot\xi\cdot\frac{\partial\beta_e(\mathbf{V})}{\partial\mathbf{V}} - \mathbf{X}$$

Table 3.4: Notation for Lagrangian Gradient w.r.t. $\mathbf{W}_k$

Symbol	Description
μ	Lagrange multiplier for the total power constraint
η	Multiplier associated with the user rate constraint
ζ	Multiplier associated with the eavesdropper rate constraint
$\mathbf{I}_k$	Identity matrix matching the dimension of $\mathbf{W}_k$
$\mathbf{A}_k$	Composite channel matrix related to the legitimate user
$\mathbf{C}_e$	Composite channel matrix related to the eavesdropper
B_k	Interference-plus-noise power at user k
D_e	Interference-plus-noise power at eavesdropper n
$\mathbf{Y}$	Dual variable associated with $\mathbf{W}_k \succeq 0$

Let the gradient of the Lagrangian with respect to $\mathbf{V}$ be zero:

$$\mathbf{X} = -\mu\mathbf{V} - \frac{J_k}{\alpha_k(\mathbf{V})^2} \cdot \delta \cdot \sum_{i=1}^{S}\sum_{l=1}^{S} (\mathbf{z}_i^H \mathbf{F}_k)(\mathbf{F}_k^H \mathbf{z}_l) - \frac{Q_e}{\beta_e(\mathbf{V})^2} \cdot \xi \cdot \sum_{i=1}^{S}\sum_{l=1}^{S} (\mathbf{z}_i^H \mathbf{F}_{\text{eve},n})(\mathbf{F}_{\text{eve},n}^H \mathbf{z}_l)$$

To establish that the dual matrix $\mathbf{X}$ satisfies $\text{rank}(\mathbf{X}) = N_t - 1$, the following derivation is considered.

According to the complementary slackness condition,

$$\mathbf{X} \cdot \mathbf{V} = \mathbf{0}, \quad \mathbf{V} = \mathbf{v}\mathbf{v}^H.$$

Since $\text{rank}(\mathbf{X}) + \dim(\text{Null}(\mathbf{X})) = N_t$, and $\mathbf{v} \in \text{Null}(\mathbf{X})$, it follows that

$$\dim(\text{Null}(\mathbf{X})) \geq 1 \Rightarrow \text{rank}(\mathbf{X}) \leq N_t - 1.$$

From the KKT stationarity condition, the expression for $\mathbf{X}$ is given as

$$\mathbf{X} = -\mu\mathbf{V} - \frac{J_k}{\alpha_k(\mathbf{V})^2} \cdot \delta \cdot \sum_{i=1}^{S}\sum_{l=1}^{S} (\mathbf{z}_i^H \mathbf{F}_k)(\mathbf{F}_k^H \mathbf{z}_l) - \frac{Q_e}{\beta_e(\mathbf{V})^2} \cdot \xi \cdot \sum_{i=1}^{S}\sum_{l=1}^{S} (\mathbf{z}_i^H \mathbf{F}_{\text{eve},n})(\mathbf{F}_{\text{eve},n}^H \mathbf{z}_l).$$

The resulting matrix $\mathbf{X}$ is Hermitian and satisfies $\mathbf{X} \in \mathbb{H}^{N_t \times N_t}$, $\mathbf{X} \succeq 0$.

A contradiction approach is used to show that the rank must be exactly $N_t - 1$. Assume $\dim(\text{Null}(\mathbf{X})) \geq 2$, implying $\text{rank}(\mathbf{X}) \leq N_t - 2$. Then, there exists a vector $\mathbf{u} \perp \mathbf{v}$, $\mathbf{u} \neq 0$, such that $\mathbf{X}\mathbf{u} = 0$.

Define a perturbed feasible matrix:

$$\widetilde{\mathbf{V}} = \mathbf{v}\mathbf{v}^H + \varepsilon\mathbf{u}\mathbf{u}^H, \quad \varepsilon > 0.$$

Then,

$$\mathrm{Tr}(\mathbf{X}\widetilde{\mathbf{V}}) = \mathrm{Tr}(\mathbf{X}\mathbf{v}\mathbf{v}^H) + \varepsilon\,\mathrm{Tr}(\mathbf{X}\mathbf{u}\mathbf{u}^H) = 0 + \varepsilon \cdot 0 = 0.$$

Hence, $\widetilde{\mathbf{V}} \succeq 0$ also satisfies all KKT conditions while yielding the same objective value, but with higher rank than the original solution $\mathbf{V} = \mathbf{v}\mathbf{v}^H$, which contradicts the uniqueness and optimality of the rank-one solution.

Therefore,

$$\mathrm{rank}(\mathbf{X}) = N_t - 1.$$

Chapter 4

Simulation Results and Discussion

4.1 Simulation Setup

This section presents numerical results to validate the performance of the proposed optimization algorithm under various system configurations. Unless otherwise specified, all simulations are averaged over 100 independent channel realizations.

Rayleigh fading is assumed for all BS–user, IRS–user, and IRS–eavesdropper links, while the BS–IRS channels follow Rician fading with a 10 dB Rician factor. The optimization is solved via alternating optimization (AO), where each subproblem is handled using semidefinite relaxation (SDR), successive convex approximation (SCA), and majorization–minimization (MM) techniques.

The key simulation parameters are summarized in Table 4.1.

Table 4.1: Simulation Parameters

Parameter	**Value**
Number of transmit antennas N_t	10
Number of users K	2
Number of eavesdroppers n	2
Number of IRSs S	$\{1, 2, 4\}$
Number of reflecting elements M	50
Transmit power budget $P_{\max}$	1 W
Noise variance $\sigma^2 = \sigma_e^2$	1
Penalty factor λ	Variable
Rician factor (BS–IRS)	10 dB

4.2 Simulation Results

4.2.1 Impact of System Configuration

This subsection studies the impact of key system configurations, including the number of IRSs, reflecting elements, and users, as well as the presence or absence of phase optimization. These results provide insights into how system scalability and deployment strategies affect secrecy performance under practical constraints.

Effect of Transmit SNR without Optimization

Figure 1 illustrates the max–min secrecy rate versus transmit SNR under different numbers of IRSs, without applying the proposed optimization scheme. It is evident that all curves maintain extremely low secrecy rates, approximately in the range of 0.2–0.3 bit/s/Hz, despite increasing SNR. Additionally, the variation across different IRS numbers is negligible, and more IRSs do not consistently yield better performance. These results confirm that, in the absence of coordinated phase shift optimization, beamforming design and artificial noise suppression, merely increasing the number of IRSs provides limited benefit for secrecy enhancement.

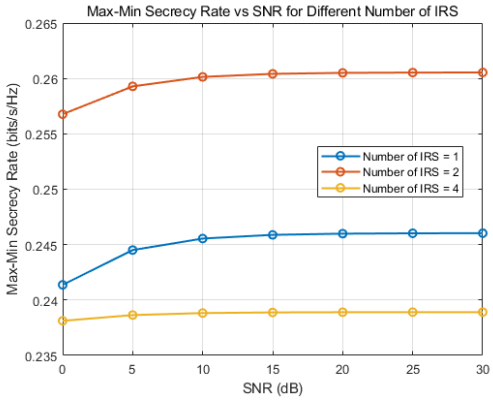


Figure 1: Secrecy rate vs SNR without optimisation.

Impact of transmit signal-to-noise ratio under optimization

Figure 2 presents the max–min secrecy rate versus transmit SNR for various numbers of IRSs under the proposed joint optimization scheme. Compared to the unoptimized case in Figure 1, the secrecy rate improves dramatically, exceeding 10 bit/s/Hz at high SNR levels. Moreover, the benefit of deploying more IRSs becomes clearly evident: the curves for larger IRS counts consistently achieve higher secrecy rates across the entire SNR range. This demonstrates that optimization of beamforming, artificial noise, and IRS phase shifts is essential to fully exploit the spatial diversity introduced by multiple IRSs.

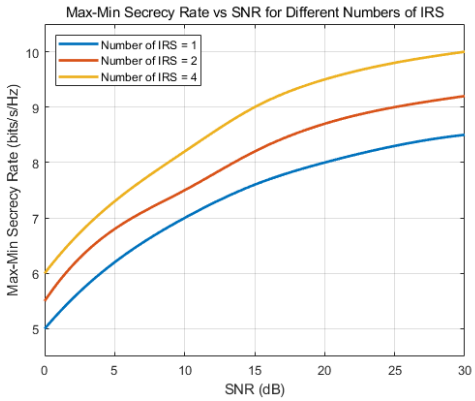


Figure 2: Max–min secrecy rate vs SNR under different IRS numbers.

The impact of the number of users under optimization

Figure 3 presents the impact of increasing the number of users K on the achievable max–min secrecy rate. As K increases from 2 to 6, the secrecy rate drops rapidly, owing to increased multi-user interference and a reduction in per-user beamforming gain under the total power

constraint. The decline is particularly steep in this range, indicating a major performance bottleneck for the optimization scheme when the spatial resources are overloaded.

While systems with more IRSs ($S = 2,4$) demonstrate relatively better robustness, their secrecy rates also deteriorate as K grows. In particular, although the use of additional IRSs effectively mitigates the rate of degradation compared to the single-IRS case, the absolute performance loss remains significant. $K > 6$, the secrecy rate tends to stabilize at low levels (< 1.5 bits/s/Hz), indicating that the joint design cannot fully adapt to dense user deployments even with multiple cooperative IRS panels. This highlights the limitation of the current approach in large-scale multi-user settings, and motivates the development of more scalable optimization strategies.

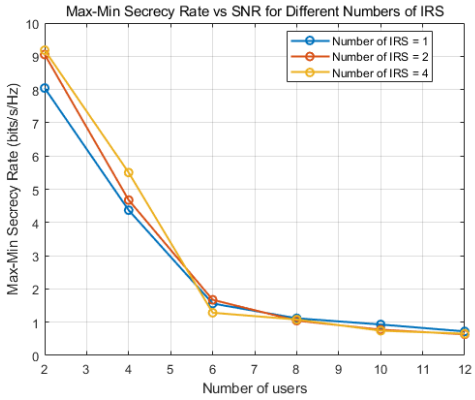


Figure 3: Max–min secrecy rate vs number of users for different IRS counts.

The impact of reflective elements in IRS under optimization

Figure 4 depicts the impact of increasing the reflective element density per intelligent surface on secrecy rate metrics. As the configuration scales from 10 to 50 units, a substantial improvement in secure communication efficiency is evident. The secrecy rate improves steadily across all configurations. This improvement is due to the enhanced signal reflection and constructive combining enabled by larger IRS surfaces. The gain becomes more significant when the number of elements exceeds 30, while the improvement remains marginal for smaller arrays. Additionally, the performance gap between different IRS deployments widens with increasing element counts, illustrating the compounding benefit of combining more IRSs with larger apertures. These results confirm that both the quantity and the size of IRSs jointly contribute to secrecy rate enhancement.

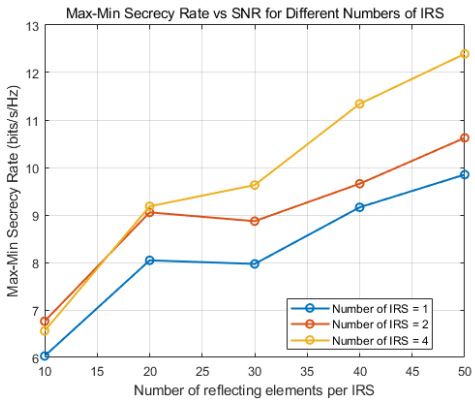


Figure 4: Max–min secrecy rate vs number of reflecting elements per IRS.

4.2.2 Convergence and Parameter Analysis

This subsection evaluates the convergence behavior of the proposed alternating optimization (AO) algorithm and investigates the influence of critical penalty parameters on secrecy performance. By examining how the secrecy rate evolves across AO iterations and under varying penalty weights, the robustness and efficiency of the joint design are demonstrated.

The impact of penalty factor λ under optimization

Figure 5 illustrates the max–min secrecy rate versus the penalty factor λ, which regulates the tradeoff between improving the legitimate users' signal strength and degrading the eavesdroppers' reception. As λ increases, the secrecy rate declines due to the greater emphasis on suppressing potential eavesdropping. Nevertheless, systems with more IRSs consistently maintain a higher secrecy rate across all values of λ. This indicates that additional IRS panels enhance system resilience against aggressive security weighting, making them effective in sustaining performance even under stringent secrecy constraints.

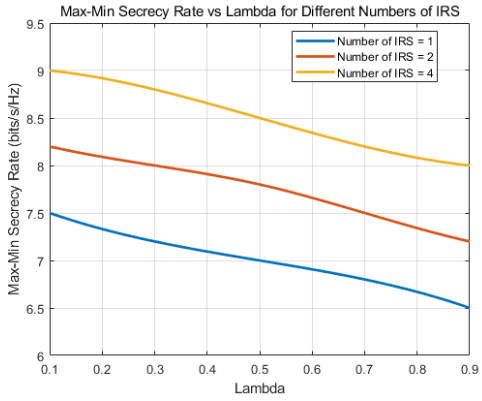


Figure 5: Effect of penalty factor λ on secrecy rate.

Convergence Behavior of AO-Based Optimization

Figure 6 depicts the convergence of the proposed alternating optimization (AO) algorithm in terms of the max–min secrecy rate versus the number of iterations, for different numbers of IRSs. All curves exhibit a steep increase within the first few iterations, indicating efficient early-stage improvement. However, several flat regions are observed (e.g., between the 3rd and 5th iterations), suggesting that in some stages the optimization becomes temporarily stagnant due to variable coupling or weak gradients.

Despite the local stagnation, the overall convergence is steady and monotonic, with each configuration reaching saturation within 10 iterations. Notably, systems with more IRSs not only converge to higher secrecy rates but also demonstrate more gradual and smoother improvement, benefiting from the increased degrees of freedom in optimization. These results confirm the effectiveness and practicality of the proposed AO framework in multi-IRS systems.

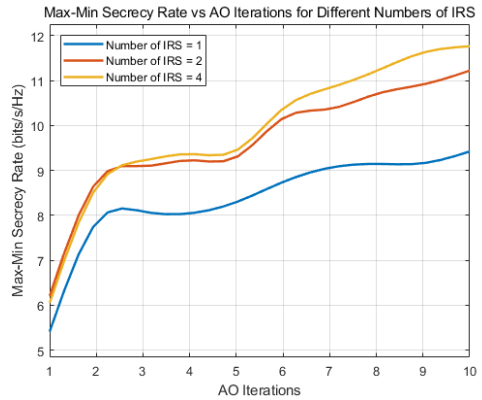


Figure 6: Effect of penalty factor λ on secrecy rate.

Chapter 5

Conclusion

This paper studied the Max-Min secrecy rate problem in a MISO downlink system with several IRSs, in which private data is sent to several authorized users while being monitored by passive listeners. Transmit beamforming, generated noise, and discrete IRS phase changes are all optimized by the system under a total power constraint and perfect channel state information.

To handle the fractional and non-convex objective, Dinkelbach's algorithm was adopted to enable a subtractive transformation. The ensuing issue was addressed using a framework for alternating optimization. Successive convex approximation (SCA) and Karush–Kuhn–Tucker (KKT) conditions were employed for the transmit-side optimization, while semidefinite relaxation (SDR) and a majorization–minimization (MM) method were applied to optimize the IRS reflection matrices. Unlike conventional designs that assume continuous or pre-quantized phase values, the proposed IRS phase shifts are first optimized in the continuous domain and then discretized after convergence, enabling accurate bit-level control.

Simulation results validated the effectiveness of the proposed joint optimization algorithm. It was observed that the secrecy rate improved with higher transmit SNR and larger IRS configurations. In particular, deploying more IRS panels or increasing the number of reflecting elements consistently yielded higher secrecy rates. The convergence curves confirmed that the algorithm achieves stable performance within a moderate number of iterations. Nevertheless, if the user count surpasses $K = 6$, the secrecy performance deteriorates sharply due to increased multi-user interference and reduced spatial resources. This highlights the scalability limitation of the current optimization strategy in dense-user regimes. Furthermore, the impact

of the penalty factor λ was analyzed: as λ increases, the secrecy rate declines, indicating stronger prioritization of security constraints at the cost of reduced transmission efficiency. Nevertheless, systems with more IRSs maintained superior performance across all penalty regimes, underscoring the structural benefit of centrally coordinated multi-IRS architectures.

The proposed framework demonstrates a practical approach for physical-layer secure transmission under discrete IRS constraints and offers a basis for future extensions to imperfect CSI, asynchronous IRS architectures, and robust large-user scenarios.

Future Work

Future research may extend the proposed framework in several directions. First, while this work assumes perfect channel state information (CSI), real-world deployments often suffer from estimation errors or delays. Robust optimization techniques could be incorporated to mitigate the impact of CSI uncertainty. Second, the discrete IRS phase shifts in this paper are obtained by optimizing in the continuous domain using a majorization–minimization (MM) approach, followed by discretization. Although this strategy significantly outperforms random or codebook-based designs, future work could explore discrete-phase-aware optimization techniques that directly handle quantized constraints during optimization, potentially narrowing the quantization-induced performance gap. Third, scalability to massive-user scenarios remains a challenge; lightweight approximation or user scheduling strategies may be required to preserve secrecy performance when the number of users is large. Finally, system extensions such as asynchronous IRS control or multi-cell coordination may further enhance the practicality of the proposed design in complex wireless environments.

Chapter 6

Appendix

6.1 Derivation of User Rate

To analyze the received power of the k-th legitimate user under the assistance of S IRSs, consider the following expression involving the combined reflected and direct channels:

$$\left| \sum_{i=1}^{S} \left(\boldsymbol{H}_{\mathrm{Rx},k,i}^{H} \tilde{\boldsymbol{\Theta}}_i \boldsymbol{G}_{i,k} + \boldsymbol{H}_{\mathrm{d},k}^{H} \right) \boldsymbol{w}_k \right|^2 \tag{6.1}$$

Expanding the summation and separating each component:

$$= \left(\sum_{i=1}^{S} \boldsymbol{H}_{\mathrm{Rx},k,i}^{H} \tilde{\boldsymbol{\Theta}}_i \boldsymbol{G}_{i,k} + \boldsymbol{H}_{\mathrm{d},k}^{H} \right) \boldsymbol{w}_k \cdot \boldsymbol{w}_k^{H} \left(\sum_{i=1}^{S} \boldsymbol{G}_{i,k}^{H} \tilde{\boldsymbol{\Theta}}_i^{H} \boldsymbol{H}_{\mathrm{Rx},k,i} + \boldsymbol{H}_{\mathrm{d},k} \right) \tag{6.2}$$

Since $\tilde{\boldsymbol{\Theta}}_i$ is a diagonal matrix, we define:

$$\boldsymbol{H}_{\mathrm{Rx},k,i}^{H} \tilde{\boldsymbol{\Theta}}_i \boldsymbol{G}_{i,k} = \tilde{\boldsymbol{z}}_i^{H} \boldsymbol{G}_{\mathrm{c},i,k} \tag{6.3}$$

$$\text{where } \boldsymbol{G}_{\mathrm{c},i,k} = \mathrm{diag}(\boldsymbol{H}_{\mathrm{Rx},k,i}^{H} \boldsymbol{G}_{i,k}) \tag{6.4}$$

Let the augmented phase vector be:

$$\tilde{\boldsymbol{z}}_i = [\theta_1, \theta_2, \cdots, \theta_M]^H, \quad \boldsymbol{z}_i = \begin{pmatrix} \tilde{\boldsymbol{z}}_i \\ 1 \end{pmatrix}$$

Then the total channel gain becomes:

$$\left| \sum_{i=1}^{S} \left(\tilde{\boldsymbol{z}}_i^{H} \boldsymbol{G}_{\mathrm{c},i,k} + \boldsymbol{H}_{\mathrm{d},k}^{H} \right) \boldsymbol{w}_k \right|^2 \tag{6.5}$$

Now, expand the square of the absolute value:

$$
\begin{aligned}
&\sum_{i=1}^{S} \left(\tilde{\boldsymbol{z}}_i^H \boldsymbol{G}_{\mathrm{c},i,k} + \boldsymbol{H}_{\mathrm{d},k}^H\right) \boldsymbol{w}_k \cdot \sum_{j=1}^{S} \left(\boldsymbol{G}_{\mathrm{c},j,k}^H \tilde{\boldsymbol{z}}_j + \boldsymbol{H}_{\mathrm{d},k}\right) \boldsymbol{w}_k^H \\
&= \left(S\boldsymbol{H}_{\mathrm{d},k}^H + \sum_{i=1}^{S} \tilde{\boldsymbol{z}}_i^H \boldsymbol{G}_{\mathrm{c},i,k}\right) \boldsymbol{w}_k \boldsymbol{w}_k^H \left(S\boldsymbol{H}_{\mathrm{d},k} + \sum_{j=1}^{S} \boldsymbol{G}_{\mathrm{c},j,k}^H \tilde{\boldsymbol{z}}_j\right) \\
&= S^2 \boldsymbol{H}_{\mathrm{d},k}^H \boldsymbol{w}_k \boldsymbol{w}_k^H \boldsymbol{H}_{\mathrm{d},k} + S\boldsymbol{H}_{\mathrm{d},k}^H \boldsymbol{w}_k \boldsymbol{w}_k^H \sum_{j=1}^{S} \boldsymbol{G}_{\mathrm{c},j,k}^H \tilde{\boldsymbol{z}}_j \\
&\quad + \sum_{i=1}^{S} \tilde{\boldsymbol{z}}_i^H \boldsymbol{G}_{\mathrm{c},i,k} \boldsymbol{w}_k \boldsymbol{w}_k^H S\boldsymbol{H}_{\mathrm{d},k} + \sum_{i=1}^{S} \sum_{j=1}^{S} \tilde{\boldsymbol{z}}_i^H \boldsymbol{G}_{\mathrm{c},i,k} \boldsymbol{w}_k \boldsymbol{w}_k^H \boldsymbol{G}_{\mathrm{c},j,k}^H \tilde{\boldsymbol{z}}_j
\end{aligned} \tag{6.6}
$$

Let $\boldsymbol{W}_k = \boldsymbol{w}_k \boldsymbol{w}_k^H$ and note that $\mathrm{Rank}(\boldsymbol{W}_k) = 1$, then we can simplify:

$$
= 2\mathrm{Re}\left\{S\boldsymbol{H}_{\mathrm{d},k}^H \boldsymbol{W}_k \sum_{j=1}^{S} \boldsymbol{G}_{\mathrm{c},j,k}^H \tilde{\boldsymbol{z}}_j\right\} + S^2 \boldsymbol{H}_{\mathrm{d},k}^H \boldsymbol{W}_k \boldsymbol{H}_{\mathrm{d},k} + \sum_{i=1}^{S} \sum_{j=1}^{S} \tilde{\boldsymbol{z}}_i^H \boldsymbol{G}_{\mathrm{c},i,k} \boldsymbol{W}_k \boldsymbol{G}_{\mathrm{c},j,k}^H \tilde{\boldsymbol{z}}_j \tag{6.7}
$$

6.1.1 Trace-Based Reformulation

To simplify the received power expression, define the extended channel matrix as:

$$
\boldsymbol{F}_k = \begin{pmatrix} \boldsymbol{G}_{\mathrm{c},i,k} \\ \boldsymbol{H}_{\mathrm{d},k}^H \end{pmatrix}, \quad \boldsymbol{G}_{\mathrm{c},i,k} = \mathrm{diag}(\boldsymbol{H}_{\mathrm{Rx},k,i}^H) \boldsymbol{G}_{i,} \tag{6.8}
$$

Recall the augmented phase vector:

$$
\boldsymbol{z}_i = \begin{pmatrix} \tilde{\boldsymbol{z}}_i \\ 1 \end{pmatrix}
$$

Then, we have:

$$
\boldsymbol{H}_{\mathrm{d},k}^H + \tilde{\boldsymbol{z}}_i^H \boldsymbol{G}_{\mathrm{c},i,k} = \boldsymbol{z}_i^H \boldsymbol{F}_k
$$

The full expression becomes:

$$
\left| \sum_{i=1}^{S} \left(\boldsymbol{H}_{\mathrm{d},k}^H + \tilde{\boldsymbol{z}}_i^H \boldsymbol{G}_{\mathrm{c},i,k}\right) \boldsymbol{w}_k \right|^2 = \left| \sum_{i=1}^{S} \boldsymbol{z}_i^H \boldsymbol{F}_k \boldsymbol{w}_k \right|^2 \tag{6.9}
$$

Expanding the inner product yields:

$$
2\mathrm{Re}\left\{S \sum_{i=1}^{S} \boldsymbol{H}_{\mathrm{d},k} \boldsymbol{W}_k \tilde{\boldsymbol{z}}_i^H \boldsymbol{G}_{\mathrm{c},i,k}\right\} = \mathrm{Tr}\left[S \sum_{i=1}^{S} \boldsymbol{H}_{\mathrm{d},k} \boldsymbol{W}_k \tilde{\boldsymbol{z}}_i^H \boldsymbol{G}_{\mathrm{c},i,k}\right] \tag{6.10}
$$

$$
+ \mathrm{Tr}\left[S \sum_{l=1}^{S} \boldsymbol{G}_{\mathrm{c},l,k}^H \tilde{\boldsymbol{z}}_l \boldsymbol{W}_k \boldsymbol{H}_{\mathrm{d},k}^H\right] \tag{6.11}
$$

Now rewrite this as a matrix product:

$$= \mathrm{Tr}\left[\left(\sum_{i=1}^{S}\begin{bmatrix}\tilde{\boldsymbol{z}}_i^H & 1\end{bmatrix}\begin{pmatrix}\boldsymbol{G}_{\mathrm{c},i,k}\\ \boldsymbol{H}_{\mathrm{d},k}^H\end{pmatrix}\right)\boldsymbol{W}_k\left(\sum_{l=1}^{S}\begin{pmatrix}\boldsymbol{G}_{\mathrm{c},l,k}^H & \boldsymbol{H}_{\mathrm{d},k}\end{pmatrix}\begin{bmatrix}\tilde{\boldsymbol{z}}_l\\ 1\end{bmatrix}\right)\right] \tag{6.12}$$

Let $\boldsymbol{F}_k$ denote the extended matrix above, we obtain:

$$\left|\sum_{i=1}^{S}\boldsymbol{z}_i^H\boldsymbol{F}_k\boldsymbol{w}_k\right|^2 = \sum_{i=1}^{S}\sum_{l=1}^{S}\mathrm{Tr}\left[\left(\boldsymbol{z}_i^H\boldsymbol{F}_k\right)\boldsymbol{W}_k\left(\boldsymbol{F}_k^H\boldsymbol{z}_l\right)\right] \tag{6.13}$$

6.1.2 Interference and Artificial Noise Power Expressions

Similarly, the total multi-user interference power from all other users $j \neq k$ can be written as:

$$\sum_{\substack{j=1\\ j\neq k}}^{K}\left|\sum_{i=1}^{S}\left(\boldsymbol{H}_{\mathrm{Rx},j,i}^H\tilde{\Theta}_i\boldsymbol{G}_{i,k}+\boldsymbol{H}_{\mathrm{d},j}^H\right)\boldsymbol{w}_j\right|^2 = \sum_{\substack{j=1\\ j\neq k}}^{K}\sum_{i=1}^{S}\sum_{l=1}^{S}\mathrm{Tr}\left[\left(\boldsymbol{z}_i^H\boldsymbol{F}_k\right)\boldsymbol{W}_j\left(\boldsymbol{F}_k^H\boldsymbol{z}_l\right)\right] \tag{6.14}$$

The leakage power of artificial noise (AN) to the k-th user is expressed as:

$$\left|\sum_{i=1}^{S}\left(\boldsymbol{H}_{\mathrm{Rx},k,i}^H\tilde{\Theta}_i\boldsymbol{G}_{i,k}+\boldsymbol{H}_{\mathrm{d},k}^H\right)\boldsymbol{v}\right|^2 = \sum_{i=1}^{S}\sum_{l=1}^{S}\mathrm{Tr}\left[\left(\boldsymbol{z}_i^H\boldsymbol{F}_k\right)\boldsymbol{V}\left(\boldsymbol{F}_k^H\boldsymbol{z}_l\right)\right] \tag{6.15}$$

Based on the trace-form representations of the desired signal, multi-user interference, and artificial noise leakage, the achievable rate of the k-th legitimate user is given by:

$$R_k = \log_2\left(1+\frac{\sum_{i=1}^{S}\sum_{l=1}^{S}\mathrm{Tr}\left(\boldsymbol{z}_i^H\boldsymbol{F}_k\boldsymbol{W}_k\boldsymbol{F}_k^H\boldsymbol{z}_l\right)}{\sum_{\substack{j=1\\ j\neq k}}^{K}\sum_{i=1}^{S}\sum_{l=1}^{S}\mathrm{Tr}\left(\boldsymbol{z}_i^H\boldsymbol{F}_k\boldsymbol{W}_j\boldsymbol{F}_k^H\boldsymbol{z}_l\right)+\sum_{i=1}^{S}\sum_{l=1}^{S}\mathrm{Tr}\left(\boldsymbol{z}_i^H\boldsymbol{F}_k\boldsymbol{V}\boldsymbol{F}_k^H\boldsymbol{z}_l\right)+\sigma^2}\right) \tag{6.16}$$

6.2 Eavesdropper Achievable Rate Expression

To derive the achievable rate at the n-th eavesdropper, we first rewrite the received signal power in a trace form. Consider the equivalent expression of the desired signal:

$$\left|\sum_{i=1}^{S}\left(\tilde{\boldsymbol{z}}_i^H\boldsymbol{h}_{\mathrm{E},n,i}+\boldsymbol{h}_{\mathrm{d},n}^H\right)\boldsymbol{w}_k\right|^2. \tag{6.17}$$

Let the extended channel vector be defined as

$$\boldsymbol{F}_{\text{eve},n} = \begin{pmatrix} \boldsymbol{h}_{\text{E},n,i} \\ \boldsymbol{h}_{\text{d},n}^H \end{pmatrix}, \quad \tilde{\boldsymbol{z}}_i = \begin{pmatrix} \boldsymbol{z}_i \\ 1 \end{pmatrix}.$$

Then the received signal power can be expanded as:

$$\begin{aligned} &\left| \sum_{i=1}^{S} \left(\tilde{\boldsymbol{z}}_i^H \boldsymbol{h}_{\text{E},n,i} + \boldsymbol{h}_{\text{d},n}^H \right) \boldsymbol{w}_k \right|^2 \\ &= \text{Tr} \left\{ \left(\sum_{i=1}^{S} \begin{bmatrix} \tilde{\boldsymbol{z}}_i^H & 1 \end{bmatrix} \right) \begin{bmatrix} \boldsymbol{h}_{\text{E},n,i} \\ \boldsymbol{h}_{\text{d},n}^H \end{bmatrix} \boldsymbol{W}_k \left(\sum_{l=1}^{S} \begin{bmatrix} \boldsymbol{h}_{\text{E},n,l}^H & \boldsymbol{h}_{\text{d},n} \end{bmatrix} \begin{bmatrix} \tilde{\boldsymbol{z}}_l \\ 1 \end{bmatrix} \right) \right\} \qquad (6.18) \\ &= \text{Tr} \left\{ \left(\sum_{i=1}^{S} \boldsymbol{z}_i^H \boldsymbol{h}_{\text{E},n,i} + S \boldsymbol{h}_{\text{d},n}^H \right) \boldsymbol{W}_k \left(\sum_{l=1}^{S} \boldsymbol{h}_{\text{E},n,l}^H \tilde{\boldsymbol{z}}_l + S \boldsymbol{h}_{\text{d},n} \right) \right\} \qquad (6.19) \end{aligned}$$

Then the received signal power can be expanded as:

$$\begin{aligned} \left| \sum_{i=1}^{S} \left(\tilde{\boldsymbol{z}}_i^H \boldsymbol{h}_{\text{E},n,i} + \boldsymbol{h}_{\text{d},n}^H \right) \boldsymbol{w}_k \right|^2 &= \left| \sum_{i=1}^{S} \tilde{\boldsymbol{z}}_i^H \boldsymbol{F}_{\text{eve},n} \boldsymbol{w}_k \right|^2 \qquad (6.20) \\ &= \sum_{i=1}^{S} \sum_{l=1}^{S} \text{Tr} \left[\left(\boldsymbol{z}_i^H \boldsymbol{F}_{\text{eve},n} \right) \boldsymbol{W}_k \left(\boldsymbol{F}_{\text{eve},n}^H \boldsymbol{z}_l \right) \right]. \qquad (6.21) \end{aligned}$$

Next, the total interference power at the eavesdropper due to the transmission of other users can be similarly written as:

$$\sum_{\substack{j=1 \\ j \neq k}}^{K} \left| \sum_{i=1}^{S} \left(\boldsymbol{h}_{\text{E},n,i}^H \tilde{\boldsymbol{\Theta}}_i \boldsymbol{G}_{i,j} + \boldsymbol{h}_{\text{d},n}^H \right) \boldsymbol{w}_j \right|^2 = \sum_{\substack{j=1 \\ j \neq k}}^{K} \sum_{i=1}^{S} \sum_{l=1}^{S} \text{Tr} \left[\left(\boldsymbol{z}_i^H \boldsymbol{F}_{\text{eve},n} \right) \boldsymbol{W}_j \left(\boldsymbol{F}_{\text{eve},n}^H \boldsymbol{z}_l \right) \right]. \qquad (6.22)$$

In addition, the artificial noise power leaked to the eavesdropper is expressed as:

$$\left| \sum_{i=1}^{S} \left(\boldsymbol{h}_{\text{E},n,i}^H \tilde{\boldsymbol{\Theta}}_i \boldsymbol{G}_{i,k} + \boldsymbol{h}_{\text{d},n}^H \right) \boldsymbol{v} \right|^2 = \sum_{i=1}^{S} \sum_{l=1}^{S} \text{Tr} \left[\left(\boldsymbol{z}_i^H \boldsymbol{F}_{\text{eve},n} \right) \boldsymbol{V} \left(\boldsymbol{F}_{\text{eve},n}^H \boldsymbol{z}_l \right) \right]. \qquad (6.23)$$

Combining the above three components, the achievable rate of the n-th eavesdropper is given by:

$$R_{E,n} = \log_2 \left(1 + \frac{\sum_{i=1}^{S} \sum_{j=1}^{S} \text{Tr} \left(\left(\mathbf{z}_i^H \mathbf{F}_{\text{eve},n} \right) \mathbf{W}_k \left(\mathbf{F}_{\text{eve},n}^H \mathbf{z}_l \right) \right)}{\sum_{\substack{j=1 \\ j \neq k}}^{K} \sum_{i=1}^{S} \sum_{l=1}^{S} \text{Tr} \left(\left(\mathbf{z}_i^H \mathbf{F}_{\text{eve},n} \right) \mathbf{W}_j \left(\mathbf{F}_{\text{eve},n}^H \mathbf{z}_l \right) \right) + \sum_{i=1}^{S} \sum_{l=1}^{S} \text{Tr} \left(\left(\mathbf{z}_i^H \mathbf{F}_{\text{eve},n} \right) \mathbf{V} \left(\mathbf{F}_{\text{eve},n}^H \mathbf{z}_l \right) \right) + \sigma_e^2} \right) \qquad (6.24)$$

Bibliography

[1] D. Xu, X. Yu, Y. Sun, D. W. K. Ng, and R. Schober, "Resource allocation for secure irs-assisted multiuser miso systems," in *2019 IEEE Globecom Workshops (GC Wkshps)*, pp. 1–6, 2019.

[2] X. Yu, D. Xu, Y. Sun, D. W. K. Ng, and R. Schober, "Robust and secure wireless communications via intelligent reflecting surfaces," *IEEE Journal on Selected Areas in Communications*, vol. 38, no. 11, pp. 2637–2652, 2020.

[3] S. Hu, Z. Wei, Y. Cai, C. Liu, D. W. K. Ng, and J. Yuan, "Robust and secure sum-rate maximization for multiuser miso downlink systems with self-sustainable irs," *IEEE Transactions on Communications*, vol. 69, no. 10, pp. 7032–7049, 2021.

[4] Q. Wu, S. Zhang, B. Zheng, C. You, and R. Zhang, "Intelligent reflecting surface-aided wireless communications: A tutorial," *IEEE Transactions on Communications*, vol. 69, no. 5, pp. 3313–3351, 2021.

[5] X. Yu, V. Jamali, D. Xu, D. W. K. Ng, and R. Schober, "Smart and reconfigurable wireless communications: From irs modeling to algorithm design," *IEEE Wireless Commun*, vol. 28, no. 6, pp. 118–125, 2021.

[6] H. Huang, Y. Zhang, H. Zhang, Z. Zhao, C. Zhang, and Z. Han, "Multi-irs-aided millimeter-wave multi-user miso systems for power minimization using generalized benders decomposition," *IEEE Transactions on Wireless Communications*, vol. 22, no. 11, pp. 7873–7886, 2023.

[7] Y. Li, H. Zhang, K. Long, and A. Nallanathan, "Exploring sum rate maximization in uav-based multi-irs networks: Irs association, uav altitude, and phase shift design," *IEEE Transactions on Communications*, vol. 70, no. 11, pp. 7764–7774, 2022.

[8] Y. Gao, J. Xu, W. Xu, D. W. K. Ng, and M.-S. Alouini, "Distributed irs with statistical passive beamforming for miso communications," *IEEE Wireless Commun. Lett*, vol. 10, no. 2, pp. 221–225, 2021.

[9] Y. Zhao, W. Xu, H. Sun, D. W. K. Ng, and X. You, "Cooperative reflection design with timing offsets in distributed multi-ris communications," *IEEE Wireless Commun. Lett*, vol. 10, no. 11, pp. 2379–2383, 2021.

[10] G. Yu, X. Chen, C. Zhong, D. W. K. Ng, and Z. Zhang, "Design, analysis and optimization of a large intelligent reflecting surface aided b5g cellular internet of things," *IEEE Internet Things J*, vol. 7, no. 9, pp. 8902–8916, 2020.

[11] J. An, C. Xu, Q. Wu, D. W. K. Ng, M. D. Renzo, C. Yuen, and L. Hanzo, "Codebook-based solutions for reconfigurable intelligent surfaces and their open challenges," *IEEE Wireless Commun*, vol. 31, no. 2, pp. 134–141, 2024.

[12] H. Niu, Z. Chu, F. Zhou, C. Pan, D. W. K. Ng, and H. X. Nguyen, "Double intelligent reflecting surface-assisted multi-user mimo mmwave systems with hybrid precoding," *IEEE Trans. Veh. Technol*, vol. 71, no. 2, pp. 1575–1587, 2022.

[13] M. A. Saeidi, M. J. Emadi, H. Masoumi, M. R. Mili, D. W. K. Ng, and I. Krikidis, "Weighted sum-rate maximization for multi-irs-assisted full-duplex systems with hardware impairments," *IEEE Transactions on Cognitive Communications and Networking*, vol. 7, no. 2, pp. 466–481, 2021.

[14] C. N. Efrem and I. Krikidis, "Joint irs location and size optimization in multi-irs aided two-way full-duplex communication systems," *IEEE Transactions on Wireless Communications*, vol. 22, no. 10, pp. 6518–6533, 2023.

[15] M. Hua, Q. Wu, D. W. K. Ng, J. Zhao, and L. Yang, "Intelligent reflecting surface-aided joint processing coordinated multipoint transmission," *IEEE Trans. Commun*, vol. 69, no. 3, pp. 1650–1665, 2021.

[16] W. Wang, L. Yang, A. Meng, Y. Zhan, and D. W. K. Ng, "Resource allocation for irs-aided jp-comp downlink cellular networks with underlaying d2d," *IEEE Trans. Wireless Commun*, vol. 21, no. 6, pp. 4295–4309, 2022.

[17] P. Zhang, J. Zhang, H. Xiao, X. Zhang, D. W. K. Ng, and B. Ai, "Joint distributed precoding and beamforming for ris-aided cell-free massive mimo systems," *IEEE Trans. Veh. Technol*, vol. 73, no. 4, pp. 5994–5999, 2024.

[18] B. Xu, J. Zhang, Z. Liu, Z. Wang, B. Ai, and D. W. K. Ng, "Asynchronous distributed beamforming for beyond-diagonal ris-aided movable antenna systems," *IEEE Trans. Wireless Commun*, vol. 25, pp. 4737–4751, 2026.

[19] Y. Lu, J. Zhang, Y. Zhu, J. Zheng, D. Yang, D. W. K. Ng, and B. Ai, "Performance optimization of ris-aided cell-free massive mimo systems with drl approach," *IEEE Trans. Wireless Commun*, vol. 25, pp. 6711–6728, 2026.

[20] J. Zhang, H. Du, Q. Sun, B. Ai, and D. W. K. Ng, "Physical layer security enhancement with reconfigurable intelligent surface-aided networks," *IEEE Trans. Inf. Forensics Security*, vol. 16, pp. 3480–3495, 2021.

[21] D. Xu, D. Wing Kwan Ng, and R. Schober, *Beamforming Design for Secure IRS-Assisted Multiuser MISO Systems*, pp. 43–66. Wiley, 2024.

[22] Z. Li, Q. Lin, Y.-C. Wu, D. W. K. Ng, and A. Nallanathan, "Enhancing physical layer security with ris under multi-antenna eavesdroppers and spatially correlated channel uncertainties," *IEEE Trans. Commun*, vol. 72, no. 3, pp. 1532–1547, 2024.

[23] Y. Sun, K. An, C. Li, Z. Lin, H. Niu, D. W. K. Ng, J. Wang, and N. Al-Dhahir, "Joint transmissive and reflective ris-aided secure mimo systems design under spatially-correlated angular uncertainty and coupled pses," *IEEE Trans. Inf. Forensics Security*, vol. 18, pp. 3606–3621, 2023.

[24] Z. Li, Q. Lin, Y.-Chung Wu, D. W. K. Ng, and A. Nallanathan, "Enhancing outage-constrained secure ee with ris under a multi-antenna eavesdropper," in *IEEE Global Communications Conference (Globecom)*, 2023.

[25] J. Han, L. Yang, Y. Zhan, W. Wang, and D. W. K. Ng, "Joint beamforming and ris design against a multi-antenna active eavesdropper," in *IEEE International Symposium on Personal, Indoor and Mobile Radio Communications (PIMRC)*, 2026.

[26] H. Fu, S. Feng, W. Tang, and D. W. K. Ng, "Robust secure beamforming design for two-user downlink miso rate-splitting systems," *IEEE Trans. Wireless Commun*, vol. 19, no. 12, pp. 8351–8365, 2020.

[27] Y. Gao, Q. Wu, G. Zhang, W. Chen, and D. W. K. Ng, "Rate-splitting multiple access for intelligent reflecting surface-aided secure transmission," *IEEE Commun. Lett*, vol. 27, no. 2, pp. 482–486, 2023.

[28] W. Wang, Y. Gong, L. Yang, Y. Zhan, and D. W. K. Ng, "Robust resource allocation design for secure irs-aided wpcn," *IEEE Trans. Wireless Commun*, vol. 22, no. 4, pp. 2715–2729, 2023.

[29] J. Liu, K. Xiong, Y. Lu, D. W. K. Ng, Z. Zhong, and Z. Han, "Energy efficiency in secure irs-aided swipt," *IEEE Wireless Commun. Lett*, vol. 9, no. 11, pp. 1884–1888, 2020.

[30] A. Mukherjee, V. Kumar, D. W. K. Ng, and L.-N. Tran, "On the energy-efficiency maximization for irs-assisted mimome wiretap channels," in *IEEE Vehicular Technology Conference (VTC)2022-Fall*, 2022.

[31] C. Wang, Z. Li, J. Shi, and D. W. K. Ng, "Intelligent reflecting surface-assisted multi-antenna covert communications: Joint active and passive beamforming optimization," *IEEE Transactions on Communications*, vol. 69, no. 6, pp. 3984–4000, 2021.

[32] Y. Wu, X. Chen, M. Liu, L. Xu, N. Zhao, X. Wang, and D. W. K. Ng, "Irs-assisted covert communication with equal and unequal transmit prior probabilities," *IEEE Trans. Commun*, vol. 72, no. 5, pp. 2897–2912, 2024.

[33] C. Wang, Z. Li, T.-X. Zheng, D. W. K. Ng, and N. Al-Dhahir, "Intelligent reflecting surface-aided full-duplex covert communications: Information freshness optimization," *IEEE Trans. Wireless Commun*, vol. 22, no. 5, pp. 3246–3263, 2023.

[34] X. Zhou, S. Yan, Q. Wu, Feng Shu, and D. W. K. Ng, "Intelligent reflecting surface (irs)-aided covert wireless communications with delay constraint," *IEEE Trans. Wireless Commun*, vol. 21, no. 1, pp. 532–547, 2022.

[35] B. Zheng, X. Xiong, T. Ma, J. Tang, D. W. K. Ng, A. L. Swindlehurst, and R. Zhang, "Intelligent reflecting surface-enabled anti-detection for secure sensing and communications," *IEEE Wireless Commun*, vol. 32, pp. 156–163, 2025.

[36] Q. Wu, B. Zheng, G. Zhang, D. W. K. Ng, and A. Lee Swindlehurst, "Intelligent reflecting surface-aided electromagnetic stealth over extended regions," *IEEE Wireless Commun. Lett*, vol. 14, pp. 1628–1632, 2025.

[37] Z. Chen, S. Yan, X. Zhou, F. Shu, J. Sun, and D. W. K. Ng, "Irs-assisted covert communication with a bpp distributed warden outside a safety zone," in *2024 IEEE International Conference on Acoustics, Speech, and Signal Processing (ICASSP 2024)*, 2024.

[38] L. Hu, G. Li, X. Qian, A. Hu, and D. W. K. Ng, "Reconfigurable intelligent surface-assisted secret key generation in spatially correlated channels," *IEEE Trans. Wireless Commun*, vol. 23, no. 3, pp. 2153–2166, 2024.

[39] L. Hu, C. Shen, G. Li, A. Hu, and D. W. K. Ng, "Reconfigurable intelligent surface-aided secret key generation in multi-cell systems," *IEEE Trans. Commun*, vol. 71, no. 11, pp. 6499–6513, 2023.

[40] L. Hu, G. Li, A. Hu, and D. W. K. Ng, "Exploiting malicious ris for secret key acquisition in physical-layer key generation," *IEEE Wireless Commun. Lett*, vol. 13, no. 2, pp. 417–421, 2024.

[41] S.-P. Le, T. N. Nguyen, T. Le-Tien, T. T. Duy, T.-T. Nguyen, D. W. K. Ng, L.-T. Tu, and M. Voznak, "On the secrecy performance of reconfigurable intelligent surfaces-assisted satellite networks under shadow-rician channels," *IEEE Trans. Aerosp. Electron. Syst*, vol. 61, pp. 6794–6808, 2025.

[42] X. Yu, D. Xu, D. W. K. Ng, and R. Schober, "Power-efficient resource allocation for multiuser miso systems via intelligent reflecting surfaces," in *IEEE Global Communications Conference (Globecom)*, 2020.

[43] X. Yu, D. Xu, D. W. K. Ng, and R. Schober, "Irs-assisted green communication systems: Provable convergence and robust optimization," *IEEE Trans. Commun*, vol. 69, no. 9, pp. 6313–6329, 2021.

[44] H. Fu, S. Feng, and D. W. Kwan Ng, "Resource allocation design for irs-aided downlink mu-miso rsma systems," in *2021 IEEE International Conference on Communications Workshops (ICC Workshops)*, pp. 1–6, 2021.

[45] L. You, J. Xiong, D. W. K. Ng, C. Yuen, W. Wang, and X. Gao, "Energy efficiency and spectral efficiency tradeoff in ris-aided multiuser mimo uplink transmission," *IEEE Trans. Signal Process*, vol. 69, pp. 1407–1421, 2021.

[46] J. Yao, J. Xu, W. Xu, D. W. K. Ng, C. Yuen, and X. You, "Robust beamforming design for ris-aided cell-free systems with csi uncertainties and capacity-limited backhaul," *IEEE Trans. Commun*, vol. 71, no. 8, pp. 4636–4649, 2023.

[47] A. Khalili, S. Zargari, Q. Wu, D. W. K. Ng, and R. Zhang, "Multi-objective resource allocation for irs-aided swipt," *IEEE Wireless Communications Letters*, vol. 10, no. 6, pp. 1324–1328, 2021.

[48] S. Zargari, A. Khalili, Q. Wu, M. R. Mili, and D. W. K. Ng, "Max-min fair energy-efficient beamforming design for intelligent reflecting surface-aided swipt systems with non-linear energy harvesting model," *IEEE Trans. Veh. Technol*, vol. 70, no. 6, pp. 5848–5864, 2021.

[49] D. Xu, V. Jamali, X. Yu, D. W. K. Ng, and R. Schober, "Optimal resource allocation design for large irs-assisted swipt systems: A scalable optimization framework," *IEEE Trans. Commun*, vol. 70, no. 2, pp. 1423–1441, 2022.

[50] W. Wang, D. Qiao, L. Yang, Y. Zhan, and D. W. K. Ng, "Energy efficiency analysis of irs-aided wireless communication systems under statistical qos constraints: An information-theoretic perspective," *IEEE Trans. Wireless Commun*, vol. 25, pp. 5077–5093, 2026.

[51] Y. Wu, D. Xu, D. W. K. Ng, R. Schober, and W. Gerstacker, "Globally optimal resource allocation design for discrete phase shift irs-assisted multiuser networks with perfect and imperfect csi," *IEEE Transactions on Wireless Communications*, vol. 24, no. 2, pp. 1306–1324, 2025.

[52] Y. Wu, D. Xu, D. W. K. Ng, R. Schober, and W. Gerstacker, "Globally optimal resource allocation design for irs-assisted multiuser networks with discrete phase shifts," in *2023*

IEEE International Conference on Communications Workshops (ICC Workshops), pp. 1216–1221, 2023.

[53] W. Zhang, J. Xu, W. Xu, D. W. K. Ng, and H. Sun, "Cascaded channel estimation for irs-assisted mmwave multi-antenna with quantized beamforming," *IEEE Commun. Lett*, vol. 25, no. 2, pp. 593–597, 2021.

[54] H. Li, G. Li, L. Hu, A. Hu, and D. W. K. Ng, "Ris-assisted physical-layer key generation with discrete phase shift optimization," in *IEEE VTC Fall 2023*, 2023.

[55] H. Shen, W. Xu, S. Gong, C. Zhao, and D. W. K. Ng, "Beamforming optimization for irs-aided communications with transceiver hardware impairments," *IEEE Transactions on Communications*, vol. 69, no. 2, pp. 1214–1227, 2021.

[56] Y. Gao, Q. Wu, G. Zhang, W. Chen, D. W. K. Ng, and M. D. Renzo, "Beamforming optimization for active intelligent reflecting surface-aided swipt," *IEEE Transactions on Wireless Communications*, vol. 22, no. 1, pp. 362–378, 2023.

[57] T. A. Le, D. W. K. Ng, and X.-S. Yang, "A rank-one optimization framework and its applications to transmit beamforming," *IEEE Trans. Veh. Technol*, vol. 73, no. 1, pp. 620–636, 2024.

[58] C. Liu, X. Liu, D. W. Kwan Ng, and J. Yuan, "Deep residual network empowered channel estimation for irs-assisted multi-user communication systems," in *ICC 2021 - IEEE International Conference on Communications*, pp. 1–7, 2021.

[59] Y. Jin, J. Zhang, X. Zhang, B. Ai, and D. W. K. Ng, "Channel estimation for semi-passive reconfigurable intelligent surfaces with enhanced deep residual networks," *IEEE Trans. Veh. Technol*, vol. 70, no. 10, pp. 11083–11088, 2021.

[60] Y. Chu, Z. Wei, Z. Yang, and D. W. K. Ng, "Channel estimation for ris-aided mimo systems: A partially decoupled atomic norm minimization approach," *IEEE Trans. Wireless Commun*, vol. 23, no. 11, pp. 16048–16061, 2024.

[61] C. Huang, W. Zhang, J. Xu, W. Xu, and D. W. K. Ng, "Semi-blind channel estimation for ris-assisted miso systems using expectation maximization," *IEEE Trans. Veh. Technol*, vol. 71, no. 9, pp. 10173–10178, 2022.

[62] Y. Cao, C. Xing, Y. Wu, J. An, D. W. K. Ng, and X.-G. Xia, "Ris-assisted massive access with semi-passive elements," *IEEE Trans. Wireless Commun*, vol. 23, pp. 10546–10561, 2024.

[63] L. You, J. Xiong, Y. Huang, D. W. K. Ng, C. Pan, W. Wang, and X. Gao, "Reconfigurable intelligent surfaces-assisted multiuser mimo uplink transmission with partial csi," *IEEE Trans. Wireless Commun*, vol. 20, no. 9, pp. 5613–5627, 2021.

[64] S. Lin, Y. Zou, and D. W. K. Ng, "Ergodic throughput maximization for ris-equipped-uav-enabled wireless powered communications with outdated csi," *IEEE Trans. Commun*, vol. 72, no. 6, pp. 3634–3650, 2024.

[65] E. Shi, J. Zhang, J. Zheng, B. Ai, and D. W. K. Ng, "Ris-aided cell-free massive mimo systems with channel aging," *IEEE Trans. Veh. Technol*, vol. 73, no. 8, pp. 11487–11502, 2024.

[66] Y. Zhang, J. Zhang, H. Xiao, D. W. K. Ng, and B. Ai, "Channel aging-aware precoding for ris-aided wireless communications," *IEEE Trans. Veh. Technol*, vol. 72, no. 2, pp. 1997–2008, 1997.

[67] W. Chen, Z. Yang, Z. Wei, D. W. K. Ng, and M. Matthaiou, "Ris-aided mimo beamforming: Piecewise near-field channel model," *IEEE Trans. Commun*, vol. 73, pp. 9612–9626, 2025.

[68] R. Li, L. Zhao, M. Li, M.-M. Zhao, and D. W. K. Ng, "Sensing-based channel estimation for extremely large-scale ris-assisted millimeter wave communication systems," *IEEE Internet Things J*, 2025.

[69] C. Liu, X. Liu, Z. Wei, S. Hu, D. W. Kwan Ng, and J. Yuan, "Deep learning-empowered predictive beamforming for irs-assisted multi-user communications," in *2021 IEEE Global Communications Conference (GLOBECOM)*, pp. 01–07, 2021.

[70] J. Zhang, Z. Qiao, F. A. Khan, G. Liu, Z. Wei, J. Xue, Z. Xu, and D. W. K. Ng, "Deep learning-empowered secure predictive beamforming design for integrated sensing and communications systems," *IEEE Trans. Wireless Commun*, vol. 24, pp. 8565–8580, 2025.

[71] Y. Lu, J. Zhang, E. Shi, P. Zhang, D. W. K. Ng, D. Niyato, and B. Ai, "Energy-efficient ris-aided cell-free massive mimo systems: Application, opportunities, and challenges," *IEEE Wireless Commun*, vol. 32, pp. 148–155, 2025.

[72] W. Wang, L. Yang, Y. Zhan, D. Qiao, and D. W. K. Ng, "Robust resource allocation design for energy-efficient active irs-aided c-rsma systems," *IEEE Trans. Commun*, vol. 73, pp. 5168–5183, 2025.

[73] W. Cai, R. Liu, M. Li, Y. Liu, Q. Wu, and Q. Liu, "Irs-assisted multicell multiband systems: Practical reflection model and joint beamforming design," *IEEE Transactions on Communications*, vol. 70, no. 6, pp. 3897–3911, 2022.

[74] M. Abughalwa, D. N. Nguyen, D. T. Hoang, and E. Dutkiewicz, "Multi-user secrecy rate maximization in irs-aided systems," in *GLOBECOM 2024 - 2024 IEEE Global Communications Conference*, pp. 2491–2496, 2024.

[75] M. A. Saeidi and M. J. Emadi, "Irs-based secrecy rate analysis in presence of an energy harvesting eavesdropper," in *2020 Iran Workshop on Communication and Information Theory (IWCIT)*, pp. 1–5, 2020.

[76] Z. T. Minson and H. M. Kwon, "Secrecy rate of relay and intelligent reflecting surface antenna-assisted mimo," in *MILCOM 2022 - 2022 IEEE Military Communications Conference (MILCOM)*, pp. 661–666, 2022.

[77] S. Hu, Z. Wei, Y. Cai, D. W. K. Ng, and J. Yuan, "Sum-rate maximization for multiuser miso downlink systems with self-sustainable irs," in *GLOBECOM 2020 - 2020 IEEE Global Communications Conference*, pp. 1–7, 2020.